

Longitudinal Oscillations of the Space Elevator Ribbon

Keivan Fardad

Department of Mechanical Engineering

McGill University, Montreal

April, 2016

A thesis submitted to McGill University in partial fulfilment of the
requirements of the degree of Master of Engineering

© Keivan Fardad, 2016

ACKNOWLEDGEMENTS

I would like to thank my supervisor Prof. Misra for his support and guidance toward finishing this thesis. His profound knowledge of Dynamics was a golden key in my learning and success.

I would like to thank my loving wife Tahereh for her encouragement and support during my research.

ABSTRACT

A space elevator could be an alternative to rockets for human access to space. Construction of a space elevator requires a material with a high tensile strength, and a low bulk density. An important aspect to consider before construction of the space elevator is the dynamics of space elevator. In this thesis, an important part of the dynamics - the longitudinal oscillations of the space elevator ribbon - is studied. Unlike previous works, a space station located at the geosynchronous altitude has been taken into account. Using discretization by assumed modes method and Lagrange approach, the equations of motion for the space elevator in the longitudinal direction are derived. These equations are nondimensionalized and then solved using MATLAB. Based on the solution of these equations, the effect of the mass of the space station on the period and amplitude of the longitudinal oscillations is examined. It is shown that if the mass of the space station increases, both the amplitude and the period of its oscillations increase. Also the effect of the change in the mass of the counterweight on the amplitude of the oscillations is studied. It is observed that the oscillation of the space station depends strongly on the mass of the counterweight. It was found that any increase in the mass of the counterweight, even by a small percentage, will result in oscillations of the space station and the amplitude of the oscillations increases. On the other hand, any decrease in the mass of the counterweight even by a small percentage will result in oscillations of the space station toward the earth, and the amplitude of the oscillations increase. Finally, the effect of the mass of the climber and its position on the longitudinal oscillations of the ribbon is studied, and the needed adjustments in the mass of the counterweight are presented. It was found that the climber as a point mass can increase the amplitude of the space station oscillations, and the amplitude of these oscillations depends on the mass and the distance of the climber from the geostationary altitude. It is also suggested that the climbers finally could become part of the counterweight or space station to provide such adjustments in the mass of the counterweight or the space station.

RÉSUMÉ

Un ascenseur spatial pourrait être une alternative aux fusées pour effectuer l'accès humain à l'espace. La construction d'un ascenseur spatial exige un matériau ayant une résistance à la traction élevée et une faible densité de masse. Un aspect important à considérer avant d'entamer la construction de l'ascenseur spatial est la dynamique de l'ascenseur spatial. Dans cette thèse, une partie importante de la dynamique – c'est-à-dire, les oscillations longitudinales du ruban de l'ascenseur spatial - est étudiée. Contrairement à des travaux antérieurs, une station spatiale située à l'altitude géosynchrone a été prise en considération. En utilisant la discrétisation par la méthode de modes hypothétiques et l'approche Lagrange, les équations de mouvement pour l'ascenseur spatial dans la direction longitudinale sont dérivées. Ces équations sont non- dimensionnalisées et puis résolues en utilisant MATLAB. Sur la base de la solution de ces équations, l'effet de la masse de la station spatiale sur la durée et l'amplitude des oscillations longitudinales est examiné. On démontre que, si la masse de la station spatiale augmente, l'amplitude et la durée de ses oscillations augmentent aussi. De plus, l'effet de la variation de la masse du contrepoids sur l'amplitude des oscillations est étudié. On remarque que l'oscillation de la station spatiale dépend fortement de la masse du contrepoids. Il a été constaté que toute augmentation de la masse du contrepoids, même par un petit pourcentage, se traduira par des oscillations de la station spatiale et l'amplitude des oscillations augmente. D'autre part, toute diminution de la masse du contrepoids, même par un petit pourcentage se traduira par des oscillations de la station spatiale vers la terre, et l'amplitude des oscillations augmente. Finalement, l'effet de la masse de l'ascenseur et sa position sur les oscillations longitudinales du ruban sont étudiés, et les ajustements nécessaires dans la masse du contrepoids sont présentés. On a constaté que l'ascenseur comme une masse ponctuelle peut augmenter l'amplitude des oscillations de la station spatiale, et l'amplitude de ces oscillations dépend de la masse et de la distance de l'ascenseur vis-à-vis l'altitude géostationnaire. Il est également suggéré que les ascenseurs pourraient finalement faire partie du contrepoids ou de la station spatiale pour fournir de tels ajustements dans la masse du contrepoids ou de la station spatiale.

TABLE OF CONTENTS

<i>Acknowledgements</i>	<i>i</i>
<i>Abstract</i>	<i>ii</i>
<i>Résumé</i>	<i>iii</i>
<i>Table of Contents</i>	<i>iv</i>
<i>List of Symbols</i>	<i>vi</i>
<i>List of Figures</i>	<i>x</i>
<i>List of Tables</i>	<i>xi</i>
Chapter 1: Introduction	1
1.1 The Concept of Space Elevator	1
1.2 Review of Literature	3
1.2.1 Review of Literature on the Space Elevator.....	3
1.2.2 Review of Literature on Space Elevator Dynamics	4
1.3 Objectives of the Thesis	6
1.4 Outline of the Thesis	6
Chapter 2: Fundamentals of Space Elevator Design	7
2.1 Description of the System	7
2.2 The System Components	7
2.2.1 The Ribbon.....	7
2.2.2 The Counterweight	10
2.2.3 The Space station.....	12
2.2.4 The Climber.....	12
Chapter 3: Dynamics of the Space Elevator Including a Space Station	14
3.1 Description of the Dynamic System	14
3.2 Energy Expressions and Equations of Motion	16
3.3 Nondimensionalized Equations of Motion in Matrix Form:	19

3.3.1	The Elements of Mass Matrix \mathcal{M} :	21
3.3.2	The Elements of Submatrices of K Matrix:	22
3.3.3	Elements of the Vector Function $\mathcal{F}q$:	24
3.3.4	The Elements of vector Bi :	24
Chapter 4: Analysis and Results		26
4.1	Analysis	26
4.2	The Effect of the Mass of the Space Station (ms) on the Period of Oscillation (T_s) of the Space Elevator	28
4.3	The Effect of the Mass of the Space Station (ms) on its Amplitude of Oscillation(As)	30
4.4	The Effect of the Mass of the Counterweight (mc) on the Amplitude of Space Station Oscillations(As)	31
4.4.1	– + 10 Percent Change in the Mass of the Counterweight	31
4.4.2	– + 5 Percent Change in the Mass of the Counterweight	33
4.5	The Effect of the Mass of the Climber (me) on the Amplitude of Space Station Oscillations(As)	35
4.6	The Effect of the Climber Position on the Space Elevator Equilibrium	38
4.7	Oscillation of the Space Station with Non-zero Initial Displacement	39
4.8	Summary of Results	41
Chapter 5: Conclusions		42
1.5	Summary of the Results	42
1.6	Suggestions for Future Study	43
References		44

LIST OF SYMBOLS

$\vec{F}_1(\vec{q})$	=	First nonlinear vector function
$\hat{F}_1(\xi_1)$	=	Taper function in terms of non-dimensional position along lower ribbon
$\vec{F}_2(\vec{q})$	=	Second nonlinear vector function
$\hat{F}_2(\xi_2)$	=	Taper function in terms of non-dimensional position along upper ribbon
\vec{B}_{1i}	=	First sub-vector of \vec{B}
\vec{B}_{2i}	=	Second sub-vector of \vec{B}
$\vec{F}(\vec{q})$	=	Nonlinear vector function of non-dimensional equation of motion
A_m	=	Maximum cross-sectional area of ribbon
A_o	=	Minimum cross-sectional area of ribbon
A	=	Cross-sectional area of the ribbon
A_1	=	Cross-sectional area of the lower ribbon
A_2	=	Cross-sectional area of the upper ribbon
A_s	=	Amplitude of space station oscillation
\vec{B}	=	Vector function of non-dimensional equation of motion
D_e	=	Non-dimensional position of climber
E	=	Modulus of elasticity of ribbon material
$F(s)$	=	Taper function in terms of position along ribbon
$F_1(s_1)$	=	Taper function in terms of position along lower ribbon
$F_2(s_2)$	=	Taper function in terms of position along upper ribbon
F_e	=	Force on climber
\mathbf{K}	=	Non-dimensional stiffness matrix
K	=	Kinetic Energy Expression
K_s	=	Kinetic energy of space station

K_C	=	Kinetic energy of counterweight
K_E	=	Kinetic energy of climber
K_{R1}	=	Kinetic energy of lower ribbon
K_{R2}	=	Kinetic energy of upper ribbon
L	=	Total length of ribbon after elongation
L_{e1}	=	Length of lower ribbon before elongation
L_{e2}	=	Length of upper ribbon before elongation
L_{1R}	=	Non-dimensional length of lower ribbon
L_{2R}	=	Non-dimensional length of upper ribbon
M_C	=	Non-dimensional mass of counterweight
M_e	=	Non-dimensional mass of climber
\mathcal{M}	=	Non-dimensional mass matrix
N	=	Number of generalized coordinates on each part of ribbon
P	=	Potential energy expression
P_S	=	Potential energy of space station
P_C	=	Potential energy of counterweight
P_E	=	Potential energy of climber
P_{EL}	=	Elastic potential energy of ribbon
P_{R1}	=	Potential energy of lower ribbon
P_{R2}	=	Potential energy of upper ribbon
Q_{1i}	=	Generalized force
Q_{2i}	=	Generalized force
R	=	Radius of Earth
R_G	=	Geosynchronous orbit radius

T_s	=	Period of space station oscillation
U_c	=	Longitudinal displacement of counterweight
Ω	=	Angular velocity of the Earth
\vec{r}_c	=	Position vector of counterweight
\vec{r}_E	=	Position vector of climber
\vec{r}_{R1}	=	Position vector of point on the lower ribbon
\vec{r}_{R2}	=	Position vector of point on the upper ribbon
\vec{r}_s	=	Position vector of space station
\vec{v}_s	=	Velocity vector of space station
\vec{v}_c	=	Velocity vector of counterweight
\vec{v}_E	=	Velocity vector of climber
\vec{v}_{R1}	=	Velocity vector of point on the lower ribbon
\vec{v}_{R2}	=	Velocity vector of point on the upper ribbon
$\hat{\rho}_m$	=	Non-dimensional maximum linear density of ribbon
a_i	=	Generalized coordinate for the lower ribbon
b_i	=	Generalized coordinate for the upper ribbon
d_b	=	Position of base
d_e	=	Position of climber along the reference line
e_h	=	Unit vector coinciding with local horizontal
e_v	=	Unit vector coinciding with local vertical
m_c	=	Mass of counterweight
m_e	=	Mass of climber
m_s	=	Mass of space station
q_i	=	Generalized coordinate

$r_e^{\Delta c}$	=	Ratio of required adjustment in mass of the counterweight to position of climber
s_1	=	Position on lower ribbon
s_2	=	Position on upper ribbon
u_1	=	Longitudinal extension of lower ribbon along reference line
u_{1H}	=	Longitudinal displacement of space station relative to GEO
u_2	=	Longitudinal extension of upper ribbon along reference line
\vec{q}	=	Non-dimensional vector of generalized coordinates
ε_0	=	Nominal strain of ribbon
ξ_1	=	Non-dimensional position on lower ribbon
ξ_2	=	Non-dimensional position on upper ribbon
ρ_m	=	Maximum linear density of ribbon
Δm_c	=	Change in mass of counterweight
h	=	Characteristic height of ribbon
A	=	Libration angle of ribbon
g	=	Surface gravity of Earth
r	=	Radial position on ribbon
s	=	Position on ribbon
t	=	Time
q	=	Non-dimensional generalized coordinate
r	=	Ratio of length of upper ribbon to lower ribbon
γ	=	Bulk density of ribbon material
μ	=	Gravitational constant of Earth
σ	=	Nominal stress in ribbon
τ	=	Non-dimensional time

LIST OF FIGURES

Figure 1.1: Schematic Model of the Space Elevator	2
Figure 2.1: Schematic Model of the Space Elevator Including the Space Station	8
Figure 3.1: Dynamics model of space elevator including space station	15
Figure 4.1: Longitudinal Oscillation of the Lower Ribbon with $ms = 50$ tons.	27
Figure 4.2: Longitudinal Oscillation of the Upper Ribbon with $ms = 50$ tons.....	28
Figure 4.3: Longitudinal Oscillation of the Space Station (u_1) for $ms = 50$ tons ($T_s=4.53$ hours, $A_s = 2.2$ km)	29
Figure 4.4: Longitudinal Oscillation of the Space Station (u_1) for $ms = 500$ tons ($T_s =$ 5.33 hours, $A_s = 3.85$ km)	29
Figure 4.5: Relative Oscillation of the Space Station with Respect to GEO (u_{1H}) for $ms =$ 200 tons; $mc = 330$ tons.....	31
Figure 4.6: Relative Oscillation of the Space Station with Respect to GEO (u_{1H}) for $ms =$ 200 tons; $mc = 300$ tons 10% decrease.....	32
Figure 4.7: Relative Oscillation of the Space Station with Respect to GEO (u_{1H}) for $ms =$ 200 tons; $mc = 360$ tons (10% increase).	33
Figure 4.8: Relative Oscillation of the Space Station with Respect to GEO (u_{1H}) for $ms =$ 200 tons; $mc = 313.5$ tons (5% decrease).	34
Figure 4.9: Relative Oscillation of the Space Station with Respect to GEO (u_{1H}) for $ms =$ 200 tons; $mc = 313.5$ tons (5% decrease).	34
Figure 4.10: Oscillation of the Space Station Relative to the GEO versus time for $me =$ 100 kg.	36
Figure 4.11: Oscillation of the Space Station Relative to the GEO versus time for $me =$ 500 kg.	37
Figure 4.12: Oscillation of the Space Station Relative to the GEO versus time for $me =$ 1000 kg.....	37
Figure 4.13: Plot of $re\Delta c$ versus de	39
Figure 4.14: Oscillation of the Space Station relative to GEO with initial Position of 40 km above the GEO.	40

LIST OF TABLES

Table 4.1: Period of Space Station Oscillation versus its Mass.	30
Table 4.2: Amplitude of Space Station Oscillation (A_s) versus its Mass (m_s)	30
Table 4.3: Amplitude of the Space Station Oscillation (A_s) Versus the Mass of the Climber (m_e).	38
Table 4.4: Summary of the Results for the Oscillation of Space Station and Counterweight	41

CHAPTER 1: INTRODUCTION

1.1 The Concept of Space Elevator

Human access to space has become possible with rockets. However, the inefficiency of this method was what motivated scientists and engineers to look for an alternative method. In the next few decades, that alternative could take the form of the space elevator.

The space elevator is composed of a very long tether (ribbon) extending from the surface of the Earth to a point beyond the geosynchronous altitude, a counterweight at the end of the ribbon, a space station at the geosynchronous altitude, and a climber (Figure 1.1). The climber can ascend the ribbon and carry the payload to space.

It has been shown that the ribbon is subjected to large tension due to the combined effect of the gravitational and centrifugal forces acting on the ribbon in opposite directions. It has been shown that a material with high enough strength-to-weight ratio is needed to build the space elevator. Conventional materials do not satisfy the requirements. Although carbon nanotube has been found to have the necessary material properties for space elevator construction, its production in large quantities is not yet possible with current technology. However, progress in this field is being made.

The possible applications of the space elevator are: 1) launching satellites into low-Earth-orbits, 2) sending payloads into parabolic or hyperbolic trajectories out of the solar system and toward other planets (Pearson 1975), 3) retrieving retired satellites and transporting them back to the Earth 4), recapturing the energy of returning spacecraft by induction and using this energy to move the climbers along the ribbon (Pearson 1975), 5) building a geostationary platform (a space station) for experimental purposes and astronomical studies (Pearson 1975) which could then be used as a control center by changing the length of the upper ribbon and 6) sending radioactive waste to the Sun to be incinerated, thereby saving the environment from the accumulation of hazardous material (Pearson 1975).

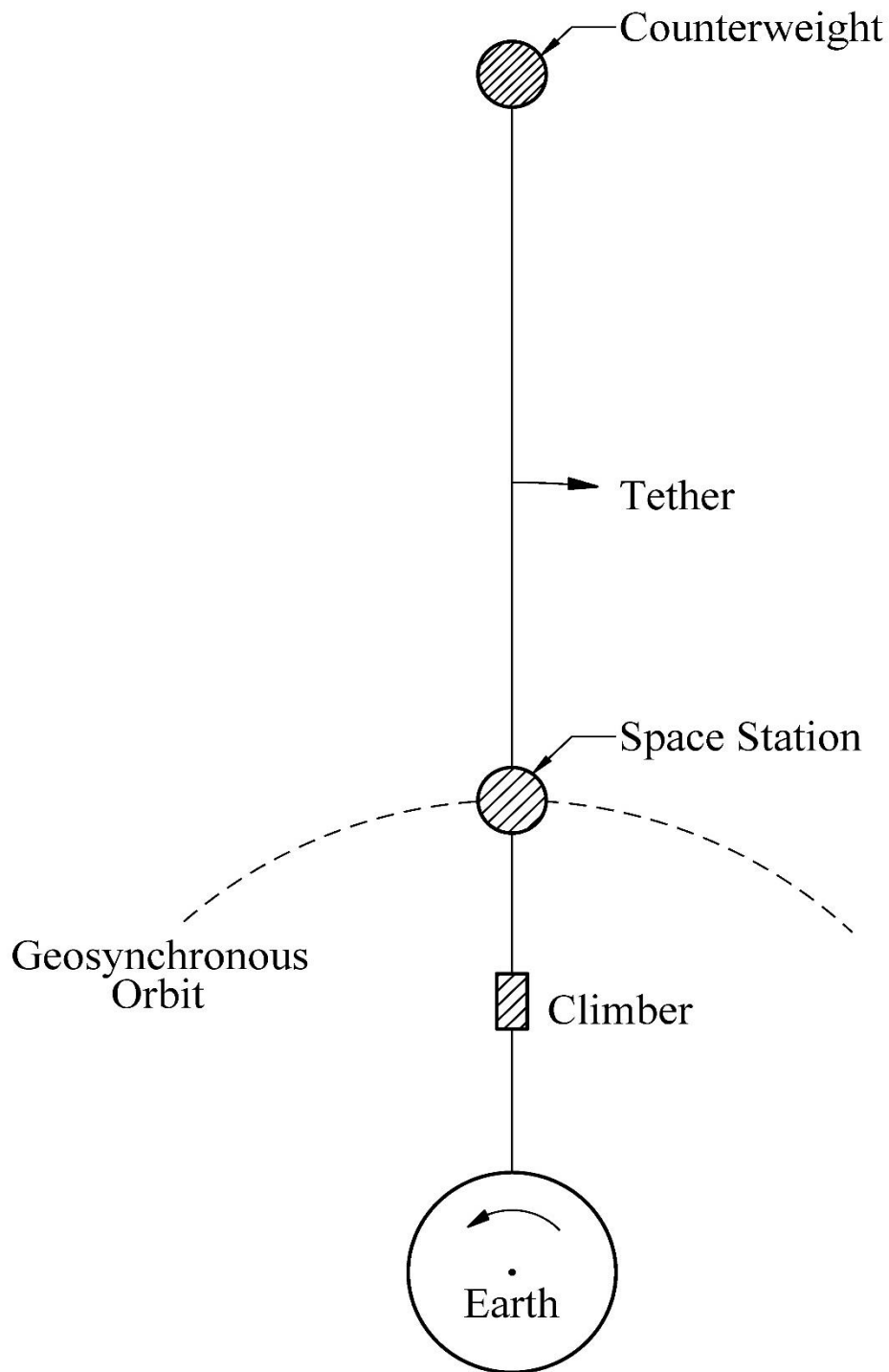


Figure 1.1: Schematic Model of the Space Elevator

It has been shown that the cost of accessing space and launching satellites with a space elevator is one hundred fold cheaper than with rockets. The use of rockets is inefficient because more than

ninety percent of the weight of the rocket is due to the fuel onboard. Also, the engines of the rockets operate very inefficiently at high velocities (Cohen and Misra 2007). The drag force of the atmosphere on the rocket also contributes to their inefficiency. The space elevator may be reused many times, and although it requires a large initial cost for construction, it will result in a larger payback over its usage life.

1.2 Review of Literature

1.2.1 Review of Literature on the Space Elevator

The idea of the space elevator was suggested for the first time by Konstantin Tsiolkovsky (1895). He imagined the space elevator as a tower under severe compression. Later, Yuri Artsutanov (1960) proposed the space elevator as a cable in tension. But the first person to address the space elevator in engineering analysis terms was Jerome Pearson (1975). In his paper, he discusses many aspects of the “orbital tower.” Pearson proves the theoretical feasibility of the construction of a space elevator in this paper. The main theoretical issues facing the orbital tower, such as buckling, strength and dynamic stability are discussed. He shows that if the length of the ribbon is about 144,000 km, the space elevator ribbon will be in equilibrium, because the gravitational and centripetal forces will balance each other. As a result, all of the ribbon will be in tension, and no buckling will occur. He also derived the equation for the required cross-sectional area of the ribbon as an exponential function of the characteristic height. He defined the characteristic height as a parameter proportional to the ratio of strength to density of the ribbon material.

The maximum cross section of the ribbon (A_m) should be at the geosynchronous altitude, and the minimum one (A_o) at the Earth. He derived also the taper ratio ($\frac{A_m}{A_o}$) as an exponential function of the characteristic height. To have a reasonable taper ratio, the characteristic height should be thousands of kilometers.

In 1975 there was no material with such a large characteristic height. In 1991 Sumio Ijima discovered a new material, a carbon nanotube made of hexagonal arrays of carbon atoms. Though this material has a characteristic height of more than 2000 km, it is not possible to produce it in large enough quantities to build a space elevator. The discovery of this nanotube lured many scientists into space elevator research.

For construction of the space elevator, Pearson suggested that the ribbon could be released from the geosynchronous orbit in two directions: one toward the Earth, and the other away from the Earth. He also showed that to avoid the tidal excitations of the moon on the tower, the taper ratio should not be lower than three.

In addition, Pearson put forth many practical applications for the orbital tower. The main application is to launch satellites via space elevator rather than via rocket; a lot of fuel is then saved. If the payload is released from a point above the GEO, it will gain enough velocity to be launched in a parabolic trajectory toward the Sun or Mercury. Also, the radioactive waste products can be sent toward the Sun. The tower can be used as a platform for experimental space research. In summary, Pearson proved the theoretical feasibility of the space elevator.

Edward (2000) addressed many practical problems about a possible space elevator. He believed that the initial ribbon should be deployed from the GEO in two directions as was suggested by Pearson. However, he suggested that in the climbing stage, the climbers ascend the ribbon and increase its thickness as they go by releasing more ribbon material; in fact, the initial ribbon should be used for its own construction. Other problems threatening the space elevator such as micrometeorites, LEO objects, and radiation damage were studied and it was shown that all of these problems are solvable by near-future technology.

1.2.2 Review of Literature on Space Elevator Dynamics

Lang (2005) showed that the Coriolis force is the main source of climber transit problems. The libration angle induced by climber transit was shown to be dependent on both the speed and the location of the climber. He also showed that the longitudinal modes of vibration would be excited by the acceleration and deceleration of the climber.

Cohen and Misra (2007) studied the elastic oscillations of the ribbon both in longitudinal and transverse directions. Using modal analysis, they found the period of the first mode for longitudinal motion to be about 5.5 h, and that of the pendulum mode to be about 6 days. The analysis of Cohen and Misra did not consider the presence of a space station at the geosynchronous altitude.

Cohen and Misra (2009) also studied the effect of climber transit on space elevator dynamics using a rigid tether approximation. They found that the climber transit has a negligible effect on the motion of the space elevator's base. The response to climber transit was found to be a sum of oscillatory terms and a linear term. It was also shown that the value of the induced libration angle

(pitch angle) is proportional to the mass of the climber and its velocity. Finally, three climbing procedures were introduced to minimize residual libration. One of these procedures was to phase multiple climbers with specific amounts of time between them. It was shown that proper phasing can eliminate residual libration, while improper phasing can result in a huge increase in residual libration and damage to the space elevator.

Williams (2009) used a lumped mass approach to derive two dynamic models for a space elevator. In the first model, he studied the dynamics of the space elevator as a result of applied forces. In the second one, he studied the space elevator kinematics. He performed a modal analysis for each model, and found that the fundamental frequency of oscillation is pendular, with a period of about 160 hours for in-plane motion and 24 hours for out-of-plane motion.

Williams and Ockels (2009) studied the dynamic minimization of in-plane librational oscillations using a rigid ribbon model. They showed that it is possible to eliminate the librational oscillations by changing the direction of the elevator for a short period of time. They also studied the out-of-plane librations, and showed that it is not possible to minimize these librations by adjustments in climber motion.

Woo and Misra (2010) presented a model for a partial space elevator considered to be floating in space and shorter in length. They modelled the space elevator as an N-body tethered system and considered only the in-plane motion. Libration frequencies were found in cases where the climber was static at the GEO altitude. Since residual librations can change the orbit of the payload launched from the climber, two methods to minimize them were introduced. The first method was to use two climbers with a specific separation in time. The second method was to use two climbers moving in opposite directions and located in mirror image about the center of mass. It was found that the residual libration and also the error in the orbit of launched payloads was less with the second method.

Cohen and Misra (2015) studied the static deformation of a space elevator when it is loaded with a climber. They used an assumed modes numerical approach. Based on the numerical results, they found that when a climber is located below the geosynchronous orbit the stress on the tether below it decreases, and the one above does not change. Conversely, when the climber is located above the geosynchronous orbit, the stress on the tether below it is increased and the one above does not

change. They also presented the plot for the displacement of the counterweight against the location of the climber.

Generally, there are three main approaches in the study of space elevator dynamics: (1) the lumped mass method, (2) the finite element method and (3) the continuum model based on the assumed modes method. In the present study, the continuum model (based on the assumed modes method) is used.

1.3 Objectives of the Thesis

The objective of this thesis is to study the longitudinal oscillations of a space elevator consisting of an elastic tether, a counterweight, a space station at the geosynchronous altitude, and a climber. The equations of motion governing the longitudinal oscillations are derived using the Lagrangian approach. Based on these equations, the following items will be examined:

- 1) The effect of the mass of the space station on the longitudinal oscillations of the space elevator, i.e., on the frequency and amplitude of the oscillations.
- 2) The effect of the mass of the space station on the amplitude of the counterweight oscillation.
- 3) The effect of the mass of the counterweight on the period and the amplitude of the space station oscillation, and on the amplitude of counterweight oscillation.

1.4 Outline of the Thesis

Chapter 2 discusses the fundamentals of the space elevator dynamical model, including a space station at the geosynchronous altitude and an elastic tether. The dimensions of the system including the length of both the upper and lower ribbons necessary for the equilibrium of the system are defined.

Chapter 3 presents the derivation of the equation of motion based on the model presented in Chapter 2 using the Lagrange approach. The assumed modes method is used for the discretization of the continuum tether. The equations of motion are nondimensionalized and presented in matrix form.

The results of the numerical solution of the nonlinear equations of motion using MATLAB are presented in Chapter 4. The effects of various system parameters on the solution are discussed.

Chapter 5 includes the summary of the results, and also gives some suggestions for future research.

CHAPTER 2: FUNDAMENTALS OF SPACE ELEVATOR DESIGN

2.1 Description of the System

The space elevator is composed of a very long tether (ribbon), a counterweight mass, a space station attached to the ribbon at the geostationary altitude, and a climber (elevator). The components of this model are presented in Figure 2.1. The lower end of the tether is connected to the Earth at a certain point on the equator, at ground level, or to an oil tanker on the ocean. The entire system rotates with angular velocity Ω (2π rad /24 hours). The motion of the lower end of the space elevator could be used to control its dynamics actively. In this study, only the longitudinal motion of the space elevator is considered.

There are three common approaches to modeling the dynamics of a cable or tether system: (1) lumped mass models, (2) finite element models, and (3) continuum models. In this study, the continuum model based on the assumed modes method will be used. Attempts have been made to determine the effects that adding a space station to the system would have on the dynamics of a space elevator. The lateral motion and the parameters such as libration angle (α), and displacement of the base (d_b) are ignored. The aerodynamic effects of the lower atmosphere are also out of the scope of this study.

2.2 The System Components

In our model, the space elevator is composed of four parts: The ribbon, the counterweight, the space station, and the climber (elevator). The details of each space elevator component are discussed below.

2.2.1 The Ribbon

The ribbon or tether has a rectangular cross section with one dimension much smaller than the other to decrease the probability of collisions with space debris and satellites. In order for the system to be in equilibrium without a counterweight, its required length is about 144,000 km. This length was calculated by Pearson (1975) for the first time. However, if the length of the ribbon is shorter than this value, it will be necessary to include a counterweight at the top to provide equilibrium. Pearson also derived the variation of the cross-sectional area to provide constant stress along the ribbon. Cohen (2006) revised the function of the cross sectional area taking into account the strain of the ribbon material (ϵ_0). The result was as follows:

$$A(r) = A_m \exp[F(r)] \quad (2.1)$$

where:

$$F(r) = \frac{R^2}{hR_G(1+\varepsilon_0)} \left[\frac{3}{2} - \frac{R_G}{r} - \frac{r^2}{2R_G^2} \right] \quad (2.2)$$

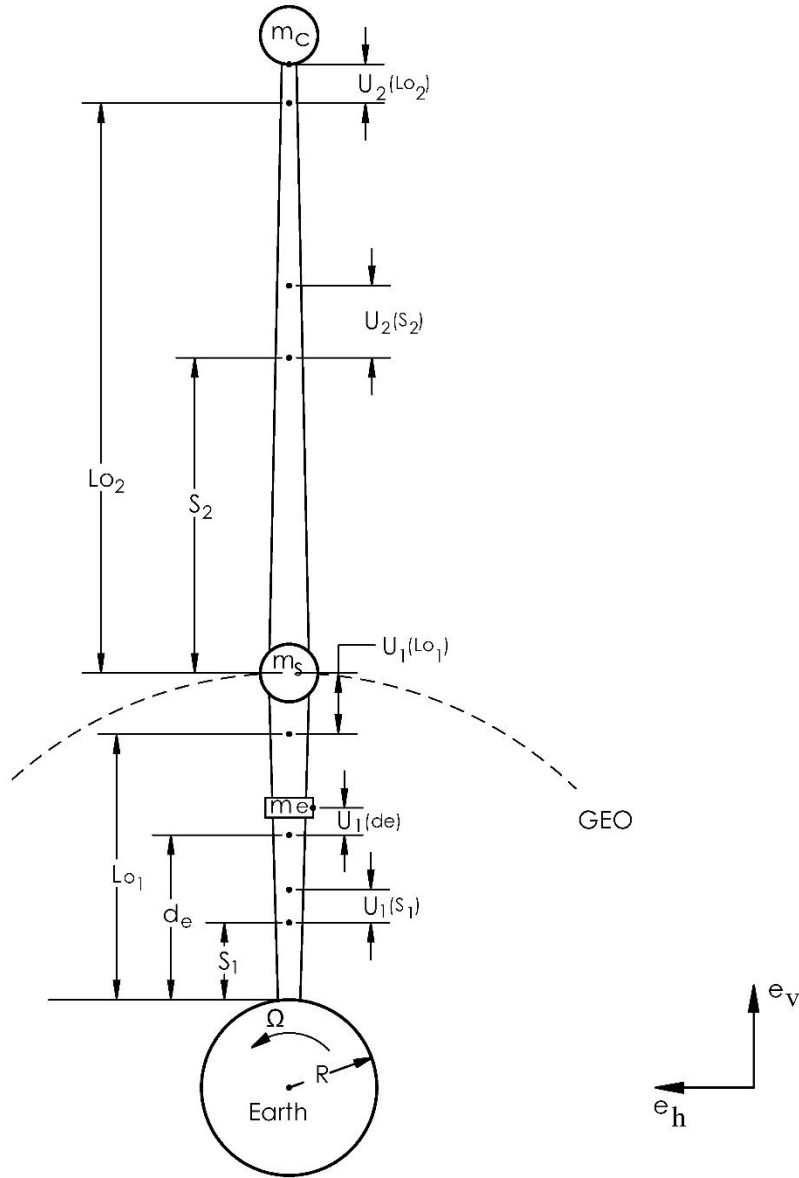


Figure 2.1: Schematic Model of the Space Elevator Including the Space Station

Here, A_m is the maximum cross-sectional area of the ribbon, r is the radial distance from the center of the earth, R_G is the radius of the geosynchronous orbit, R is the radius of the earth, and h is the

characteristic height of the ribbon material. The characteristic height which is a property of the ribbon material is defined as the strength to specific weight ratio of the ribbon material in meters:

$$h = \frac{\sigma}{\gamma g} \quad (2.3)$$

where σ and γ are the tensile strength and bulk density of the ribbon material respectively, and g is the gravitational acceleration at the earth's surface.

Assuming constant bulk density for the ribbon material (γ), the linear density function of the ribbon $\rho(s)$ is given by (Cohen and Misra 2007):

$$\rho(s) = \gamma A_m \exp[F(s)] \quad (2.4)$$

where:

$$F(s) = \frac{R^2}{hR_G(1+\varepsilon_0)} \left[\frac{3}{2} - \frac{R_G}{R+s(1+\varepsilon_0)} - \frac{[R+s(1+\varepsilon_0)]^2}{2R_G^2} \right] \quad (2.5)$$

Here, s is the longitudinal distance along the ribbon from the Earth surface.

In this model, the ribbon is composed of two parts: the lower ribbon (below the GEO to the space station) and the upper ribbon (above the GEO).

The cross sectional area function for both parts of the ribbon is defined as follows:

$$A_1(s_1) = A_m \exp[F_1(s_1)] \quad (2.10)$$

$$A_2(s_2) = A_m \exp[F_2(s_2)] \quad (2.11)$$

where:

$$F_1(s_1) = \frac{R^2}{hR_G(1+\varepsilon_0)} \left[\frac{3}{2} - \frac{R_G}{R+s_1(1+\varepsilon_0)} - \frac{[R+s_1(1+\varepsilon_0)]^2}{2R_G^2} \right] \quad (2.7)$$

$$F_2(s_2) = \frac{R^2}{hR_G(1+\varepsilon_0)} \left[\frac{3}{2} - \frac{R_G}{R+(L_{o1}+s_2)(1+\varepsilon_0)} - \frac{[R+(L_{o1}+s_2)(1+\varepsilon_0)]^2}{2R_G^2} \right] \quad (2.9)$$

The maximum cross sectional area of the ribbon (A_m) happens to be at the geosynchronous orbit where the gravitational force ($\frac{\mu}{r^2}$) and the centripetal force ($r\Omega^2$) are equal.

Therefore, the functions of the linear density for each part of the ribbon can be written separately based on the proper coordinate:

$$\rho_1(s_1) = \gamma A_m \exp[F_1(s_1)] \quad (2.6)$$

$$\rho_2(s_2) = \gamma A_m \exp[F_2(s_2)] \quad (2.8)$$

Here, s_1 and s_2 are the longitudinal distances from the Earth's surface (along the lower ribbon), and from the space station (along the upper ribbon) respectively (Figure 2.1). Also, L_{o1} and L_{o2} are the initial lengths of the lower and upper ribbons, respectively.

Most of the mass of the space elevator is due to the ribbon. If the ribbon has a characteristic height of 2750 km (carbon nanotube) and maximum cross sectional area of $A_m = 10 \text{ mm}^2$, the mass of the ribbon will be more than 900 tons.

The taper ratio is defined as the ratio of A_m (maximum cross sectional area) to A_o (cross sectional area at the earth) as follows:

$$\frac{A_m}{A_o} = \exp \left[\frac{R}{h(1+\varepsilon_0)} \left(1 - \frac{R}{R_G} \right)^2 \left(1 + \frac{R}{2R_G} \right) \right] \quad (2.12)$$

The taper ratio of the ribbon is highly dependent on the characteristic height of the ribbon material.

If the properties of carbon nanotube are considered, the characteristic height will be $h = 2750 \text{ km}$ and the taper ratio will be about 6, which is a reasonable value.

The ribbon will be at high tension (350 kN at the geosynchronous altitude) due to opposing forces acting in opposite directions: the gravitational force and the centripetal force. At a point below the geosynchronous orbit, the gravitational force is dominant. But, at a point above the geosynchronous orbit, the centripetal force is dominant. At the geosynchronous orbit, these opposing forces are equal. Pearson (1975) calculated that if the length of the ribbon were about 144,000 km, the system would be in equilibrium.

Pearson (1975) has calculated that the first longitudinal vibration period of the ribbon will last approximately 5.5 hours. This value will be investigated in our more accurate study. Edward (2000) has suggested "variations in the location of the counterweight mass, and active damping at the anchor of this mode could be used to eliminate the oscillation." This fact will also be verified in the present study.

2.2.2 The Counterweight

Since it was necessary to maintain uniform stress along all points of the ribbon, and since the cross sectional area at the end of the ribbon cannot be zero, a counterweight was considered to be

attached at the end of the ribbon. Taking into account the strain of the ribbon (ε_0), the mass of the counterweight (m_c) has also been revised to as follows (Cohen and Misra 2007):

$$m_c = \gamma A_m h \frac{\exp[F(s)]|_{s=L_0}}{\left(\frac{R}{R_G}\right)^2 \left[\frac{R+L}{R_G} - \left(\frac{R_G}{R+L}\right)^2\right]} \quad (2.13)$$

where $F(s)$ is defined by equation 2.5. Here, L_0 is the unstretched length of the total ribbon such that $L_0 = L_{o1} + L_{o2}$, and L is the total length of the ribbon after elongation, i.e.,:

$$L = L_{o1}(1 + \varepsilon_0) + L_{o2}(1 + \varepsilon_0) \quad (2.14)$$

The mass of the counterweight is proportional to the maximum cross section of the ribbon. On the other hand, the mass of the counterweight depends on the total length of the space elevator. The shorter the length of the ribbon, the higher the mass of the counterweight needed to provide equilibrium. This fact gives us a freedom in the design of a space elevator in terms of total length and the mass of the counterweight. As the length of the total ribbon approaches $R_G - R$, the mass of the counterweight needed for equilibrium approaches infinity.

For the initial ribbon, the maximum cross section is considered to be 10 mm^2 . Based on this, along with the measurement of the carbon nanotube ribbon, $100,000 \text{ km}$ in length (after elongation due to strain), the mass of the counterweight is found to be about 330 tons. These values will be used in our study. But for the total length of about $144,000 \text{ km}$, the mass of the counterweight will be about 50 tons.

Since we require that the space station at the static equilibrium be located at the geosynchronous altitude, we have found the initial length of lower and upper ribbons as follows:

First the total length of $L = 100,000 \text{ km}$ (after elongation due to strain) is chosen, such that it matches with the mass of the counterweight of 330 tons (Equation 2.13). Then, considering the strain value of ribbon material (carbon nanotube) and based on these equations:

$$L_{o1} = (R_G - R)/(1 + \varepsilon_0) \quad (2.15)$$

$$L_{o1}(1 + \varepsilon_0) + L_{o2}(1 + \varepsilon_0) = L \quad (2.16)$$

We find the following values which are used throughout this study:

$$L_{o1} = 34617 \text{ km}$$

$$L_{o2} = 62001 \text{ km}$$

2.2.3 The Space station

It is general agreement that the space elevator could not be built up from the ground. In fact, an acceptable construction scenario is as follows: a spacecraft will carry the wound ribbon to the geostationary orbit. Then the ribbon will be released in two directions (earthward and spaceward) (Edward 2000). The lower end of the ribbon will then be connected to an oil tanker on the earth. Edward (2000) has suggested that the original spacecraft moves along the spaceward ribbon to form the counterweight at the end of the ribbon. We consider the location of a space station at the geostationary orbit in the final design form of the space elevator. Therefore, part of the original spacecraft could be sent along the ribbon to form the counterweight, and the rest of the spacecraft remains at the geostationary orbit to form the space station.

In this study, the motion of the space station and its oscillation will be investigated. If the space station is located exactly at the geosynchronous altitude, the net force there will be zero, because at this level the gravitational and centrifugal effects are equal and act in opposite directions. Any disturbance from this position will induce a force on the space station pointing away from its equilibrium position. Considering the huge lumped mass of the space station, the induced force due to deviation from the equilibrium position will not be negligible. Accordingly, the equilibrium position of the space elevator will be unstable.

The level of strain on the ribbon is considerable, and based on the strength of carbon nanotube ($\sigma = 35 \text{ Gpa}$), with a safety factor of 2, and its modulus of elasticity ($E = 1000 \text{ Gpa}$), we will have $\varepsilon_0 = \frac{\sigma}{E} = 0.035$. Therefore the initial length of the lower ribbon (L_{o1}) should be chosen such that after elongation, the space station will be located at the geosynchronous orbit (Equation 2.15). This fact is considered in the analysis of this study.

2.2.4 The Climber

The climber can ascend along the ribbon to carry payloads and also to thicken the initial ribbon. It can release the payloads at the geosynchronous altitude or at points above this orbit. Releasing the payload above the geosynchronous altitude can launch it into a hyperbolic or parabolic trajectory toward other planets. It has been suggested that the climber become part of the counterweight at the end of its trajectory along the ribbon. In the design examined here, some of the climbers become part of the counterweight mass and some become part of the space station to provide the desired mass for the counterweight and the space station.

The presence of the climber on the ribbon will put extra force on the ribbon. Considering this effect, an upper limit for the mass of the climber has also been found (Cohen and Misra 2007). The climber can ascend along the ribbon with an electric motor, and laser power beaming, microwave energy, or solar energy can provide the energy for its motion. However, beyond the geosynchronous orbit, the climber can ascend the ribbon due to excess orbital energy. The speed and the mass of the climber can affect the dynamics of the space elevator.

The distance of the climber from the Earth's surface (d_e) is considered fixed in this study. The climber is assumed to be fixed at a point on the lower ribbon ($d_e = 20000 \text{ km}$). Considering the small mass of the climber compared to the total mass of the system, it is believed that its effect on the dynamics of the space elevator would be negligible. The mass of the climber was taken to be 500 kg in this study, while the mass of the counterweight is 330 tons and the mass of the ribbon is about 990 tons. The static longitudinal deflection of the climber due to strain is not ignored.

CHAPTER 3: DYNAMICS OF THE SPACE ELEVATOR INCLUDING A SPACE STATION

3.1 Description of the Dynamic System

The Space elevator system studied in this chapter is composed of five main parts: 1) the lower ribbon with the initial length L_{\circ_1} (below the GEO), 2) the upper ribbon with the initial length L_{\circ_2} (above the GEO), 3) the space station with the mass m_s located at the GEO, 4) the counterweight with the mass m_c attached at the end point of the upper ribbon, and 5) the climber with the mass m_e located at a point along the ribbon.

A simple model of the space elevator is shown in figure 3.1. In this system, only the longitudinal displacement of the space elevator is studied. The coordinate axes $i = e_v$ and $j = e_h$ point in the local vertical and horizontal directions respectively. The tether is assumed to have a finite modulus of elasticity (E), and therefore, the strain in the tether is found according to $\varepsilon_0 = \frac{\sigma}{E}$.

The positions of elements on the lower and upper ribbons are defined as s_1 and s_2 measured from the earth and the space station respectively. The assumed modes method (Meirovitch 1997) is used to study the dynamics of the system. The displacement of elements located at s_1 and s_2 are described by $u_1(t, s_1)$ and $u_2(t, s_2)$ respectively as follows:

$$u_1(t, s_1) = \varepsilon_0 s_1 + \sum_{i=1}^N a_i(t) \Phi_{1i}(s_1) \quad (3.1)$$

$$u_2(t, s_2) = \varepsilon_0 s_2 + \sum_{i=1}^N b_i(t) \Phi_{2i}(s_2) \quad (3.2)$$

The variables $a_i(t)$ and $b_i(t)$ are $N + N = 2N$ generalized coordinates while $\Phi_{1i}(s_1)$ and $\Phi_{2i}(s_2)$ are spatial basis functions chosen here:

$$\Phi_{1i}(s_1) = \sin \left[\frac{\left(i - \frac{1}{2}\right) \pi s_1}{L_{\circ_1}} \right] \quad (3.3)$$

$$\Phi_{2i}(s_2) = \sin \left[\frac{\left(i - \frac{1}{2}\right) \pi s_2}{L_{\circ_2}} \right] \quad (3.4)$$

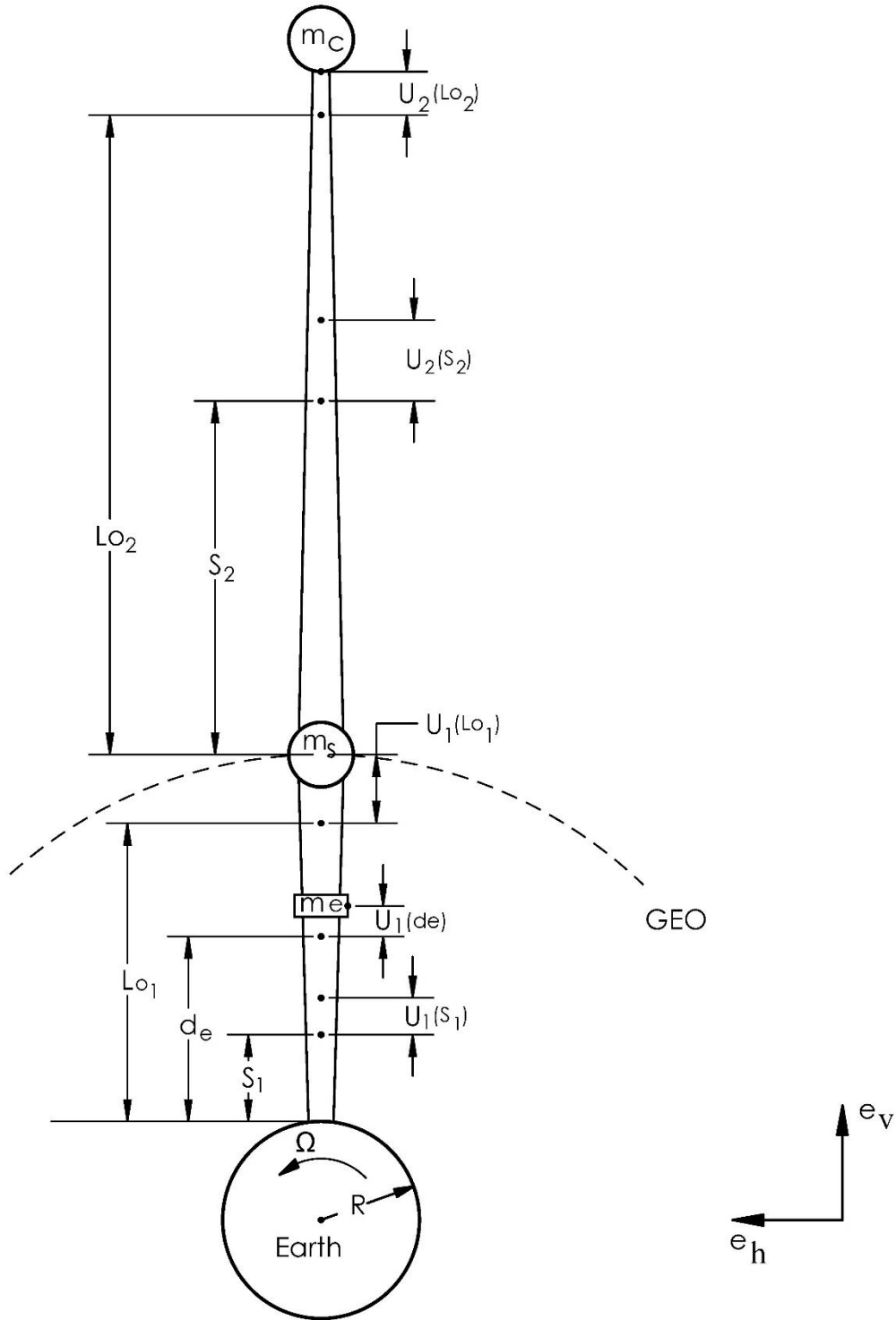


Figure 3.1: Dynamics model of space elevator including space station

These basis functions are chosen in such a way to satisfy the boundary conditions $u_1(t, 0) = 0$ and $u_2(t, 0) = 0$. Also, according to these basis functions the boundary values $u_1(t, L_{o1})$, and

$u_2(t, L_{o2})$ will be nonzero, to provide freedom of motion in lateral directions for the space station and the counterweight.

It has been assumed that after elongation of the lower ribbon, the space station will be at the geosynchronous orbit. To satisfy this condition, the initial length of the lower ribbon (L_{o1}) is chosen as follows:

$$L_{o1} = \frac{R_G - R}{1 + \varepsilon_0} \quad (3.5)$$

Where: R_G is the geosynchronous radius, and R is the earth radius.

3.2 Energy Expressions and Equations of Motion

The dynamic equations of motion for the system are derived using Lagrange approach. To do this, first, the equations of kinetic and potential energy of the system should be derived.

The position vectors for the components of the system are as follows:

$$\vec{r}_E = (R + d_e + u_1(d_e))\vec{i} \quad (3.6)$$

$$\vec{r}_{R1} = (R + s_1 + u_1)\vec{i} \quad (3.7)$$

$$\vec{r}_S = (R + L_{o1} + u_1(L_{o1}))\vec{i} \quad (3.8)$$

$$\vec{r}_{R2} = (R + L_{o1} + u_1(L_{o1}) + s_2 + u_2)\vec{i} \quad (3.9)$$

$$\vec{r}_C = (R + L_{o1} + u_1(L_{o1}) + L_{o2} + u_2(L_{o2}))\vec{i} \quad (3.10)$$

The subscripts E , $R1$, S , $R2$, and C show the elevator, lower ribbon, space station, upper ribbon, and counterweight respectively.

The velocity vectors are as follows:

$$\vec{v}_E = (0)\vec{i} + [\Omega(R + d_e + u_1(d_e))]\vec{j} \quad (3.11)$$

$$\vec{v}_{R1} = (\dot{u}_1)\vec{i} + [\Omega(R + s_1 + u_1)]\vec{j} \quad (3.12)$$

$$\vec{v}_S = [\dot{u}_1(L_{o1})]\vec{i} + [\Omega(R + L_{o1} + u_1(L_{o1}))]\vec{j} \quad (3.13)$$

$$\vec{v}_{R2} = [\dot{u}_1(L_{o1}) + \dot{u}_2]\vec{i} + [\Omega(R + L_{o1} + u_1(L_{o1}) + s_2 + u_2)]\vec{j} \quad (3.14)$$

$$\vec{v}_C = [\dot{u}_1(L_{o1}) + \dot{u}_2(L_{o2})]\vec{i} + [\Omega(R + L_{o1} + u_1(L_{o1}) + L_{o2} + u_2(L_{o2}))]\vec{j} \quad (3.15)$$

The kinetic energy of the space elevator components are as follows:

$$K_E = \frac{1}{2} m_e (\vec{v}_E \cdot \vec{v}_E) \quad (3.16)$$

$$K_{R1} = \frac{1}{2} \int_0^{L_{\circ 1}} \rho_1(s_1) [\vec{v}_{R1}(s_1) \cdot \vec{v}_{R1}(s_1)] ds_1 \quad (3.17)$$

$$K_S = \frac{1}{2} m_s (\vec{v}_S \cdot \vec{v}_S) \quad (3.18)$$

$$K_{R2} = \frac{1}{2} \int_0^{L_{\circ 2}} \rho_2(s_2) [\vec{v}_{R2}(s_2) \cdot \vec{v}_{R2}(s_2)] ds_2 \quad (3.19)$$

$$K_C = \frac{1}{2} m_c (\vec{v}_C \cdot \vec{v}_C) \quad (3.20)$$

Therefore, the total kinetic energy of the system is:

$$K = K_E + K_{R1} + K_S + K_{R2} + K_C \quad (3.21)$$

The potential energy of the space elevator components are as follows:

$$P_E = \frac{-\mu m_e}{\sqrt{\vec{r}_E \cdot \vec{r}_E}} \quad (3.22)$$

$$P_{R1} = -\mu \int_0^{L_{\circ 1}} \frac{\rho_1(s_1)}{\sqrt{\vec{r}_{R1}(s_1) \cdot \vec{r}_{R1}(s_1)}} ds_1 \quad (3.23)$$

$$P_S = \frac{-\mu m_s}{\sqrt{\vec{r}_S \cdot \vec{r}_S}} \quad (3.24)$$

$$P_{R2} = -\mu \int_0^{L_{\circ 2}} \frac{\rho_2(s_2)}{\sqrt{\vec{r}_{R2}(s_2) \cdot \vec{r}_{R2}(s_2)}} ds_2 \quad (3.25)$$

$$P_C = \frac{-\mu m_c}{\sqrt{\vec{r}_C \cdot \vec{r}_C}} \quad (3.26)$$

$$P_{EL} = \frac{1}{2} E \int_0^{L_{\circ 1}} A_1(s_1) \left(\frac{\partial u_1}{\partial s_1} \right)^2 ds_1 + \frac{1}{2} E \int_0^{L_{\circ 2}} A_2(s_2) \left(\frac{\partial u_2}{\partial s_2} \right)^2 ds_2 \quad (3.27)$$

where:

$$\frac{\partial u_1}{\partial s_1} = \varepsilon_0 + \sum_{i=1}^N \frac{\pi \left(i - \frac{1}{2} \right)}{L_{\circ 1}} a_i(t) \cos \left[\frac{\left(i - \frac{1}{2} \right) \pi s_1}{L_{\circ 1}} \right] \quad (3.28)$$

$$\frac{\partial u_2}{\partial s_2} = \varepsilon_0 + \sum_{i=1}^N \frac{\pi \left(i - \frac{1}{2} \right)}{L_{\circ 2}} b_i(t) \cos \left[\frac{\left(i - \frac{1}{2} \right) \pi s_2}{L_{\circ 2}} \right] \quad (3.29)$$

Here, the P_{EL} shows the elastic potential energy of the ribbon.

Therefore, the total potential energy of the system is:

$$P = P_E + P_{R1} + P_S + P_{R2} + P_C + P_{EL} \quad (3.30)$$

The generalized coordinates are a_i ($i = 1 \dots N$) and b_i ($i = 1 \dots N$). $N + N = 2N$ equations of motion are derived using Lagrange equation:

$$\frac{\partial}{\partial t} \left(\frac{\partial K}{\partial \dot{a}_i} \right) - \frac{\partial K}{\partial a_i} + \frac{\partial P}{\partial a_i} = Q_{1i} \quad i = 1 \dots N \quad (3.31)$$

$$\frac{\partial}{\partial t} \left(\frac{\partial K}{\partial \dot{b}_i} \right) - \frac{\partial K}{\partial b_i} + \frac{\partial P}{\partial b_i} = Q_{2i} \quad i = 1 \dots N \quad (3.32)$$

where Q_{1i} and Q_{2i} are the generalized forces on the lower and upper ribbons respectively.

The equations of motion are obtained as follows:

$$\begin{aligned} & \int_0^{L_{o1}} \rho_1(s_1) \ddot{u}_1 \phi_{1i}(s_1) ds_1 + m_s \ddot{u}_1(L_{o1}) (-1)^{i+1} \\ & + \int_0^{L_{o2}} \rho_2(s_2) [\ddot{u}_1(L_{o1}) + \ddot{u}_2] (-1)^{i+1} ds_2 \\ & + m_c [\ddot{u}_1(L_{o1}) + \ddot{u}_2(L_{o2})] (-1)^{i+1} \\ & - m_e \Omega^2 [R + d_e + u_1(d_e)] \phi_{1i}(d_e) \\ & - \int_0^{L_{o1}} \rho_1(s_1) \Omega^2 [R + s_1 + u_1] \phi_{1i}(s_1) ds_1 \\ & - m_s \Omega^2 [R + L_{o1} + u_1(L_{o1})] (-1)^{i+1} \\ & - \int_0^{L_{o2}} \rho_2(s_2) \Omega^2 [R + L_{o1} + u_1(L_{o1}) + s_2 + u_2] (-1)^{i+1} ds_2 \\ & - m_c \Omega^2 [R + L_{o1} + u_1(L_{o1}) + L_{o2} + u_2(L_{o2})] (-1)^{i+1} \\ & + \frac{\mu m_e \phi_{1i}(d_e)}{[R + d_e + u_1(d_e)]^2} + \mu \int_0^{L_{o1}} \frac{\rho_1(s_1) \phi_{1i}(s_1)}{[R + s_1 + u_1]^2} ds_1 \\ & + \frac{\mu m_s (-1)^{i+1}}{[R + L_{o1} + u_1(L_{o1})]^2} + \mu \int_0^{L_{o2}} \frac{\rho_2(s_2) (-1)^{i+1}}{[R + L_{o1} + u_1(L_{o1}) + s_2 + u_2]^2} ds_2 \\ & + \frac{\mu m_c (-1)^{i+1}}{[R + L_{o1} + u_1(L_{o1}) + L_{o2} + u_2(L_{o2})]^2} + E \int_0^{L_{o1}} A_1(s_1) u_{1s} \frac{\partial u_{1s}}{\partial a_i} ds_1 = 0 \end{aligned} \quad (3.33)$$

where:

$$u_{1s} = \frac{\partial u_1}{\partial s_1} = \varepsilon_0 + \sum_{i=1}^N \frac{\pi(i-\frac{1}{2})}{L_{o1}} a_i(t) \cos \left[\frac{(i-\frac{1}{2})\pi s_1}{L_{o1}} \right] \quad (3.34)$$

$$\frac{\partial u_{1s}}{\partial a_i} = \frac{\pi(i-\frac{1}{2})}{L_{o1}} \cos \left[\frac{(i-\frac{1}{2})\pi s_1}{L_{o1}} \right] \quad (3.35)$$

$$\begin{aligned}
& \int_0^{L^{\circ 2}} \rho_2(s_2)[\ddot{u}_1(L^{\circ 1}) + \ddot{u}_2] \phi_{2i}(s_2) ds_2 \\
& - \int_0^{L^{\circ 2}} \rho_2(s_2) \Omega^2 [R + L^{\circ 1} + u_1(L^{\circ 1}) + s_2 + u_2] \phi_{2i}(s_2) ds_2 \\
& + m_C [\ddot{u}_1(L^{\circ 1}) + \ddot{u}_2(L^{\circ 2})] (-1)^{i+1} \\
& - m_C \Omega^2 [R + L^{\circ 1} + u_1(L^{\circ 1}) + L^{\circ 2} + u_2(L^{\circ 2})] (-1)^{i+1} \\
& + \mu \int_0^{L^{\circ 2}} \frac{\rho_2(s_2) \phi_{2i}(s_2)}{[R + L^{\circ 1} + u_1(L^{\circ 1}) + s_2 + u_2]^2} ds_2 \\
& + \frac{\mu m_C (-1)^{i+1}}{[R + L^{\circ 1} + u_1(L^{\circ 1}) + L^{\circ 2} + u_2(L^{\circ 2})]^2} \\
& + E \int_0^{L^{\circ 2}} A_2(s_2) u_{2s} \frac{\partial u_{2s}}{\partial b_i} ds_2 = 0
\end{aligned} \tag{3.36}$$

where:

$$u_{2s} = \frac{\partial u_2}{\partial s_2} = \varepsilon_0 + \sum_{i=1}^N \frac{\pi(i-\frac{1}{2})}{L^{\circ 1}} b_i(t) \cos \left[\frac{(i-\frac{1}{2})\pi s_2}{L^{\circ 2}} \right] \tag{3.37}$$

$$\frac{\partial u_{2s}}{\partial b_i} = \frac{\pi(i-\frac{1}{2})}{L^{\circ 2}} \cos \left[\frac{(i-\frac{1}{2})\pi s_2}{L^{\circ 2}} \right] \tag{3.38}$$

The generalized forces acting on the system can be due to: 1) aerodynamic forces acting on the lower parts of the first ribbon, and 2) trust forces due to the motion of the climber along the ribbon. Both of these forces are neglected in this study, and the generalized forces are assumed to be zero.

3.3 Nondimensionalized Equations of Motion in Matrix Form:

The parameters of the equations are nondimensionalized based on the following definitions:

$$\xi_1 = \frac{s_1}{L^{\circ 1}} \tag{3.39}$$

$$\xi_2 = \frac{s_2}{L^{\circ 2}} \tag{3.40}$$

$$M_C = \frac{m_C}{m_s} \tag{3.41}$$

$$M_e = \frac{m_e}{m_s} \tag{3.42}$$

$$\Lambda = \frac{EA_m}{m_s \Omega^2 L^{\circ 1}} \tag{3.43}$$

$$\lambda = \frac{\mu}{R^3 \Omega^2} \tag{3.44}$$

$$L_{1R} = \frac{L^{\circ_1}}{R} \quad (3.45)$$

$$L_{2R} = \frac{L^{\circ_2}}{R} \quad (3.46)$$

$$D_e = \frac{d_e}{R} \quad (3.47)$$

$$\mathbf{r} = \frac{L^{\circ_2}}{L^{\circ_1}} \quad (3.48)$$

$$\tau = \Omega t \quad (3.49)$$

$$\mathbf{q} = \frac{q}{R} \quad (3.50)$$

$$\hat{\rho}_m = \rho_m \cdot \frac{L^{\circ_1}}{m_s} \quad (3.51)$$

$$\mathbf{q}'' = \frac{1}{R\Omega^2} \ddot{q} \quad (3.52)$$

where q is defined as:

$$a_i = q_i \quad i = 1 \dots N$$

$$b_i = q_{i+N} \quad i = 1 \dots N$$

τ is the nondimensionalized time.

The nondimensionalized basis functions are as follows:

$$\hat{\phi}_i(\xi_1) = \sin \left[\left(i - \frac{1}{2} \right) \pi \xi_1 \right] \quad (3.53)$$

$$\hat{\phi}_i(\xi_2) = \sin \left[\left(i - \frac{1}{2} \right) \pi \xi_2 \right] \quad (3.54)$$

The nondimensionalized taper functions for the lower and upper ribbons respectively are as follows:

$$\hat{\mathcal{F}}_1(\xi_1) = \frac{R^2}{hR_G(1+\varepsilon_0)} \left[\frac{3}{2} - \frac{R_G}{R+L^{\circ_1}\xi_1(1+\varepsilon_0)} - \frac{[R+L^{\circ_1}\xi_1(1+\varepsilon_0)]^2}{2R_G^2} \right] \quad (3.55)$$

$$\hat{\mathcal{F}}_2(\xi_2) = \frac{R^2}{hR_G(1+\varepsilon_0)} \left[\frac{3}{2} - \frac{R_G}{R+(L^{\circ_1}+L^{\circ_2}\xi_2)(1+\varepsilon_0)} - \frac{[R+(L^{\circ_1}+L^{\circ_2}\xi_2)(1+\varepsilon_0)]^2}{2R_G^2} \right] \quad (3.56)$$

The nondimensionalized equation of motion in matrix form is found to be:

$$\mathcal{M}\vec{q}'' + \mathbf{K}\vec{q} + \vec{\mathcal{F}}(\vec{q}) = \vec{\mathbf{B}} \quad (3.57)$$

The mass matrix \mathcal{M} is the nondimensionalized mass matrix with $2N \times 2N$ dimension. It is composed of four $N \times N$ submatrices:

$$\mathcal{M} = \begin{bmatrix} \mathcal{M}_{11} & \vdots & \mathcal{M}_{12} \\ \cdots & \vdots & \cdots \\ \mathcal{M}_{21} & \vdots & \mathcal{M}_{22} \end{bmatrix} \quad (3.58)$$

The stiffness matrix \mathbf{K} is the nondimensionalized stiffness matrix with $2N \times 2N$ dimension. It is composed of four $N \times N$ submatrices:

$$\mathbf{K} = \begin{bmatrix} \mathbf{K}_{11} & \vdots & \mathbf{K}_{12} \\ \cdots & \vdots & \cdots \\ \mathbf{K}_{21} & \vdots & \mathbf{K}_{22} \end{bmatrix} \quad (3.59)$$

The vector function $\vec{\mathcal{F}}(\vec{q})$ is a $2N \times 1$ vector of \vec{q} , which is a nonlinear function of \vec{q} .

The vector $\vec{\mathbf{B}}$ ($2N \times 1$) is independent of \vec{q} .

The vector of generalized coordinates is written as:

$$\vec{q} = [q_1, q_2, \dots, q_N, q_{N+1}, \dots, q_{2N}]^T \quad (3.60)$$

The first N generalized coordinates (q_1, q_2, \dots, q_N) are the nondimensionalized forms of a_i , corresponding to the lower ribbon, and the second N generalized coordinates (q_{N+1}, \dots, q_{2N}) are the nondimensionalized forms of b_i , corresponding to the upper ribbon.

3.3.1 The Elements of Mass Matrix \mathcal{M} :

The elements of the submatrices of \mathcal{M} are defined as follows:

$$\mathcal{M}_{11} = [m_{i,j}^{1,1}] \quad (3.61)$$

$$i = 1, 2, \dots, N$$

$$j = 1, 2, \dots, N$$

where:

$$m_{i,j}^{1,1} = \hat{\rho}_m \int_0^1 \hat{\phi}_i(\xi_1) \hat{\phi}_j(\xi_1) \exp[\hat{\mathcal{F}}_1(\xi_1)] d\xi_1 + (1 + M_c)(-1)^{i+j} + (-1)^{i+j} \hat{\rho}_m r \int_0^1 \exp[\hat{\mathcal{F}}_2(\xi_2)] d\xi_2 \quad (3.62)$$

$$\mathcal{M}_{12} = [m_{i,j}^{1,2}] \quad (3.63)$$

$$i = 1, 2, \dots, N$$

$$j = N + 1, \dots, 2N$$

where:

$$m_{i,j}^{1,2} = M_c(-1)^{i+j} + (-1)^{i+1} \hat{\rho}_m \mathbf{r} \int_0^1 \hat{\phi}_j(\xi_2) \exp[\hat{\mathcal{F}}_2(\xi_2)] d\xi_2 \quad (3.64)$$

$$\mathcal{M}_{21} = [m_{i,j}^{2,1}] \quad (3.65)$$

$$i = N + 1, \dots, 2N$$

$$j = 1, 2, \dots, N$$

where:

$$m_{i,j}^{2,1} = (-1)^{i+1} \hat{\rho}_m \mathbf{r} \int_0^1 \exp[\hat{\mathcal{F}}_2(\xi_2)] \hat{\phi}_i(\xi_2) d\xi_2 + M_c(-1)^{i+j} \quad (3.66)$$

$$\mathcal{M}_{22} = [m_{i,j}^{2,2}] \quad (3.67)$$

$$i = N + 1, \dots, 2N$$

$$j = N + 1, \dots, 2N$$

where:

$$m_{i,j}^{2,2} = \hat{\rho}_m \mathbf{r} \int_0^1 \hat{\phi}_i(\xi_2) \hat{\phi}_j(\xi_2) \exp[\hat{\mathcal{F}}_2(\xi_2)] d\xi_2 + M_c(-1)^{i+j} \quad (3.68)$$

3.3.2 The Elements of Submatrices of K Matrix:

The elements of the submatrices of K are found as follows:

$$\mathbf{K}_{11} = [k_{i,j}^{1,1}] \quad (3.69)$$

$$i = 1, 2, \dots, N$$

$$j = 1, 2, \dots, N$$

where:

$$k_{i,j}^{1,1} = -M_e \hat{\phi}_i(D_e) \hat{\phi}_j(D_e) - \hat{\rho}_m \int_0^1 \hat{\phi}_i(\xi_1) \hat{\phi}_j(\xi_1) \exp[\hat{\mathcal{F}}_1(\xi_1)] d\xi_1$$

$$\begin{aligned}
& -(1 + M_c)(-1)^{i+j} - \hat{\rho}_m \mathbf{r} \int_0^1 \exp[\hat{\mathcal{F}}_2(\xi_2)] (-1)^{i+j} d\xi_2 \\
& + \Lambda \int_0^1 \exp[\hat{\mathcal{F}}_1(\xi_1)] \pi^2 (i - \frac{1}{2})(j - \frac{1}{2}) \cos[(i - \frac{1}{2})\pi\xi_1] \cos[(j - \frac{1}{2})\pi\xi_1] d\xi_1
\end{aligned} \tag{3.70}$$

$$\mathbf{K}_{12} = [k_{i,j}^{1,2}] \tag{3.71}$$

$$i = 1, 2, \dots, N$$

$$j = N + 1, \dots, 2N$$

where:

$$k_{i,j}^{1,2} = -\hat{\rho}_m \mathbf{r} \int_0^1 \exp[\hat{\mathcal{F}}_2(\xi_2)] \hat{\phi}_j(\xi_2) (-1)^{i+1} d\xi_2 - M_c (-1)^{i+j} \tag{3.72}$$

$$\mathbf{K}_{21} = [k_{i,j}^{2,1}] \tag{3.73}$$

$$i = N + 1, \dots, 2N$$

$$j = 1, 2, \dots, N$$

where:

$$k_{i,j}^{2,1} = -(-1)^{j+1} \hat{\rho}_m \mathbf{r} \int_0^1 \hat{\mathcal{F}}_2(\xi_2) \hat{\phi}_i(\xi_2) d\xi_2 - M_c (-1)^{i+j} \tag{3.74}$$

$$\mathbf{K}_{22} = [k_{i,j}^{2,2}] \tag{3.75}$$

$$i = N + 1, \dots, 2N$$

$$j = N + 1, \dots, 2N$$

where:

$$\begin{aligned}
k_{i,j}^{2,2} &= -\hat{\rho}_m \mathbf{r} \int_0^1 \hat{\phi}_i(\xi_2) \hat{\phi}_j(\xi_2) \exp[\hat{\mathcal{F}}_2(\xi_2)] d\xi_2 - M_c (-1)^{i+j} \\
& + \frac{\Lambda}{r} \int_0^1 \exp[\hat{\mathcal{F}}_2(\xi_2)] \pi^2 (i - \frac{1}{2})(j - \frac{1}{2}) \cos[(i - \frac{1}{2})\pi\xi_2] \cos[(j - \frac{1}{2})\pi\xi_2] d\xi_2
\end{aligned} \tag{3.76}$$

3.3.3 Elements of the Vector Function $\vec{\mathcal{F}}(\vec{q})$:

The nondimensionalized vector function $\vec{\mathcal{F}}(\vec{q})$ which is nonlinear in terms of \vec{q} is composed of 2 sub-vectors as follows:

$$\vec{\mathcal{F}}(\vec{q}) = \begin{pmatrix} \vec{\mathcal{F}}_1(\vec{q}) \\ \dots \\ \vec{\mathcal{F}}_2(\vec{q}) \end{pmatrix} \quad (3.77)$$

$$\vec{\mathcal{F}}_1(\vec{q}_1) = \{f_{1i}(\vec{q})\} \quad (3.78)$$

$$i = 1, 2, \dots, N$$

where:

$$\begin{aligned} f_{1i}(\vec{q}) &= \frac{\lambda M_e \hat{\phi}_i(D_e)}{\left[1 + L_{1R} D_e + \varepsilon_0 L_{1R} D_e + \sum_{j=1}^N \mathbf{q}_j \hat{\phi}_j(D_e)\right]^2} + \int_0^1 \frac{\lambda \hat{\rho}_m \exp[\hat{\mathcal{F}}_1(\xi_1)] \hat{\phi}_i(\xi_1)}{\left[1 + (1 + \varepsilon_0) L_{1R} \xi_1 + \sum_{j=1}^N \mathbf{q}_j \hat{\phi}_j(\xi_1)\right]^2} d\xi_1 \\ &+ \frac{\lambda (-1)^{i+1}}{\left[1 + (1 + \varepsilon_0) L_{1R} + \sum_{j=1}^N (-1)^{j+1} \mathbf{q}_j\right]^2} \\ &+ \int_0^1 \frac{\lambda r \hat{\rho}_m \exp[\hat{\mathcal{F}}_2(\xi_2)] (-1)^{i+1}}{\left[1 + L_{1R}(1 + \varepsilon_0) + L_{2R} \xi_2 (1 + \varepsilon_0) + \sum_{j=1}^N \mathbf{q}_j (-1)^{j+1} + \sum_{j=N+1}^{2N} \mathbf{q}_j \hat{\phi}_j(\xi_2)\right]^2} d\xi_2 \\ &+ \frac{\lambda M_C (-1)^{i+1}}{\left[1 + (1 + \varepsilon_0) L_{1R} + (1 + \varepsilon_0) L_{2R} + \sum_{j=1}^N (-1)^{j+1} \mathbf{q}_j + \sum_{j=N+1}^{2N} (-1)^{j+1} \mathbf{q}_j\right]^2} \end{aligned} \quad (3.79)$$

$$\vec{\mathcal{F}}_2(\vec{q}) = \{f_{2i}(\vec{q})\} \quad (3.80)$$

where:

$$\begin{aligned} f_{2i}(\vec{q}) &= \int_0^1 \frac{\lambda \hat{\rho}_m r \exp[\hat{\mathcal{F}}_2(\xi_2)] \hat{\phi}_i(\xi_2)}{\left[1 + L_{1R}(1 + \varepsilon_0) + \sum_{j=1}^N \mathbf{q}_j (-1)^{j+1} + (1 + \varepsilon_0) L_{2R} \xi_2 + \sum_{j=N+1}^{2N} \mathbf{q}_j \hat{\phi}_j(\xi_2)\right]^2} d\xi_2 \\ &+ \frac{\lambda M_C (-1)^{i+1}}{\left[1 + L_{1R}(1 + \varepsilon_0) + L_{2R}(1 + \varepsilon_0) + \sum_{j=1}^N \mathbf{q}_j (-1)^{j+1} + \sum_{j=N+1}^{2N} \mathbf{q}_j (-1)^{j+1}\right]^2} \end{aligned} \quad (3.81)$$

3.3.4 The Elements of vector $\vec{\mathbf{B}}_i$:

The nondimensionalized vector $\vec{\mathbf{B}}_i$ is composed of 2 sub-vectors as follows:

$$\vec{\mathbf{B}}_i = \begin{pmatrix} \vec{\mathbf{B}}_{1i} \\ \dots \\ \vec{\mathbf{B}}_{2i} \end{pmatrix} \quad (3.82)$$

$$\vec{\mathbf{B}}_{1i} = \{b_{1i}\}_{Nx1} \quad (3.83)$$

where:

$$\begin{aligned} b_{1i} &= M_e(1 + L_{1R}D_e)\hat{\phi}_i(D_e) + M_eL_{1R}\varepsilon_0D_e\hat{\phi}_i(D_e) \\ &+ \int_0^1 \hat{\rho}_m \exp[\hat{\mathcal{F}}_1(\xi_1)][1 + L_{1R}\xi_1(1 + \varepsilon_0)] \hat{\phi}_i(\xi_1)d\xi_1 + [1 + L_{1R}(1 + \varepsilon_0)](-1)^{i+1} \\ &+ \int_0^1 \mathbf{r}\hat{\rho}_m \exp[\hat{\mathcal{F}}_2(\xi_2)][1 + L_{1R}\xi_1(1 + \varepsilon_0) + L_{2R}\xi_2(1 + \varepsilon_0)] (-1)^{i+1}d\xi_2 \\ &+ M_C[1 + (L_{1R} + L_{2R})(1 + \varepsilon_0)](-1)^{i+1} \\ &- \int_0^1 \Lambda L_{1R} \exp[\hat{\mathcal{F}}_1(\xi_1)]\varepsilon_0\pi(i - \frac{1}{2}) \cos[(i - \frac{1}{2})\pi\xi_1] d\xi_1 \end{aligned} \quad (3.84)$$

$$\vec{\mathbf{B}}_{2i} = \{b_{2i}\}_{Nx1} \quad (3.85)$$

where:

$$\begin{aligned} b_{2i} &= \int_0^1 \mathbf{r}\hat{\rho}_m \exp[\hat{\mathcal{F}}_2(\xi_2)][1 + L_{1R}(1 + \varepsilon_0) + L_{2R}\xi_2(1 + \varepsilon_0)] \hat{\phi}_i(\xi_2)d\xi_2 \\ &+ M_C[1 + (L_{1R} + L_{2R})(1 + \varepsilon_0)](-1)^{i+1} \\ &- \int_0^1 \Lambda L_{1R} \exp[\hat{\mathcal{F}}_2(\xi_2)]\varepsilon_0\pi(i - \frac{1}{2}) \cos[(i - \frac{1}{2})\pi\xi_2] d\xi_2 \end{aligned} \quad (3.86)$$

All quantities in the equations of motion in page 21 have now been determined. The equations will be solved numerically using MATLAB.

CHAPTER 4: ANALYSIS AND RESULTS

4.1 Analysis

The nondimensionalized equations of motion in matrix form (Equation 3.57) are solved using the ode45 function of MATLAB. All the initial values of generalized coordinates (q_i) and their first derivative are set to zero. The dimensions of the matrices are chosen as $2N = 10$ ($N = 5$). Based on the equation 4.1, the mass of the counterweight is set at 330 tons, to be consistent with the total length of the ribbon after elongation ($L= 100000$ km), and its maximum cross sectional area ($A_m = 10 \text{ mm}^2$). It was found that the system converges by $N=5$.

$$m_c = \gamma A_m h \frac{\exp[F(s)]|_{s=L_0}}{\left(\frac{R}{R_G}\right)^2 \left[\frac{R+L}{R_G} - \left(\frac{R_G}{R+L}\right)^2\right]} \quad (4.1)$$

The characteristic height is placed at $h = 2750$ km, and the maximum cross sectional area of the ribbon is $A_m = 10 \text{ mm}^2$. The generalized coordinate values are found for 24 hours ($\tau = 0 : 2\pi$).

Using the values of generalized coordinates for lower and upper ribbons, the following longitudinal motions are plotted for 24 hours ($\tau = 0 : 2\pi$):

- 1) Absolute longitudinal motion of the space station (u_1) versus time.
- 2) Longitudinal motion of the counterweight relative to the space station (u_2) (upper ribbon), versus time.
- 3) Absolute longitudinal motion of the counterweight (U_c) versus time.
- 4) Longitudinal motion of the space station relative to GEO (u_{1H}) versus time.

The plots are repeated for several masses of space station: 50 tons, 100 tons, 200 tons, 300 tons, 400 tons, and 500 tons.

Since we have chosen the mass of the counterweight consistent with the total length and maximum cross sectional area of the ribbon (Equation 4.1), and also the space station is initially at the geostationary orbit, it was expected that the amplitude of the oscillation of the space station and the counterweight to be negligible. However, the plots show that the space station has an oscillation with the amplitude of 2.2 km (for $m_s = 50$ tons) to 3.85km (for $m_s = 500$ tons) which depends on the mass of the space station.

The oscillations are below the geosynchronous orbit such that their maximum points are at the geosynchronous orbit. This observation can be explained by the fact that the mass of the counterweight should have been placed at a higher value by a small percentage, and also that the initials have been set to zero.

Another observation is that the amplitude of the upper ribbon's oscillations is much smaller than that of the lower ribbon regardless of the space station's mass. For example, when the mass of the space station is 50 tons, the amplitude of the oscillation of the upper ribbon is only about 0.075 km, but the amplitude of the oscillation of the lower ribbon is about 2.2 km (Figures 4.1, 4.2).

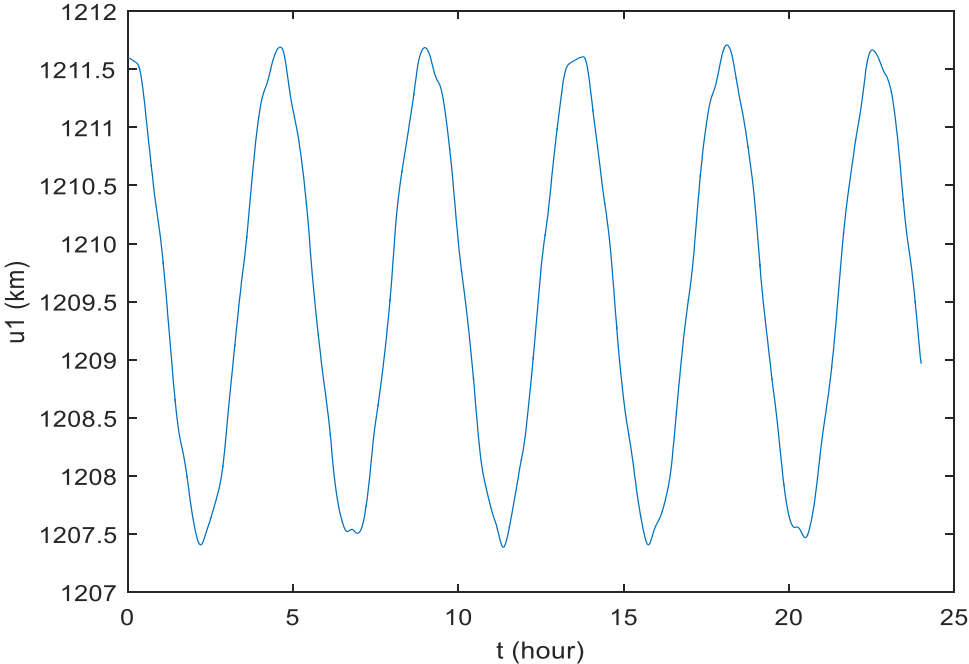


Figure 4.1: Longitudinal Oscillation of the Lower Ribbon with $m_s = 50$ tons.

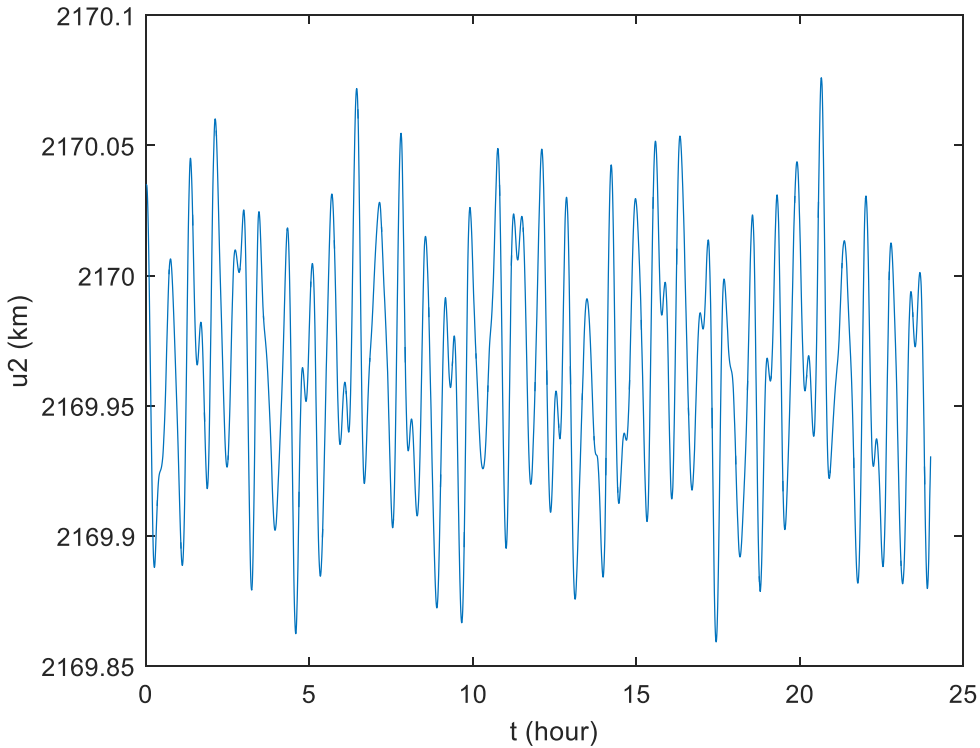


Figure 4.2: Longitudinal Oscillation of the Upper Ribbon with $m_s = 50$ tons.

The absolute displacement of the counterweight (U_c) is the sum of the displacement of the space station (due to the oscillation of the lower ribbon) (u_1), and the displacement of the upper ribbon (u_2). However, the contribution of the oscillation of the lower ribbon is much more significant than that of the upper ribbon. The absolute oscillation of the space station is equal to the oscillation of the lower ribbon at its end point (u_1).

4.2 The Effect of the Mass of the Space Station (m_s) on the Period of Oscillation (T_s) of the Space Elevator

The first observation is that as the mass of the space station is increased, the period of longitudinal oscillations increases. For example, when the mass of the space station is set to 50 tons, the period of the oscillations is observed to be about 4.53 hours. With a 500-ton space station mass, this period increases to about 5.33 hours (Figures 4.3 and 4.4).

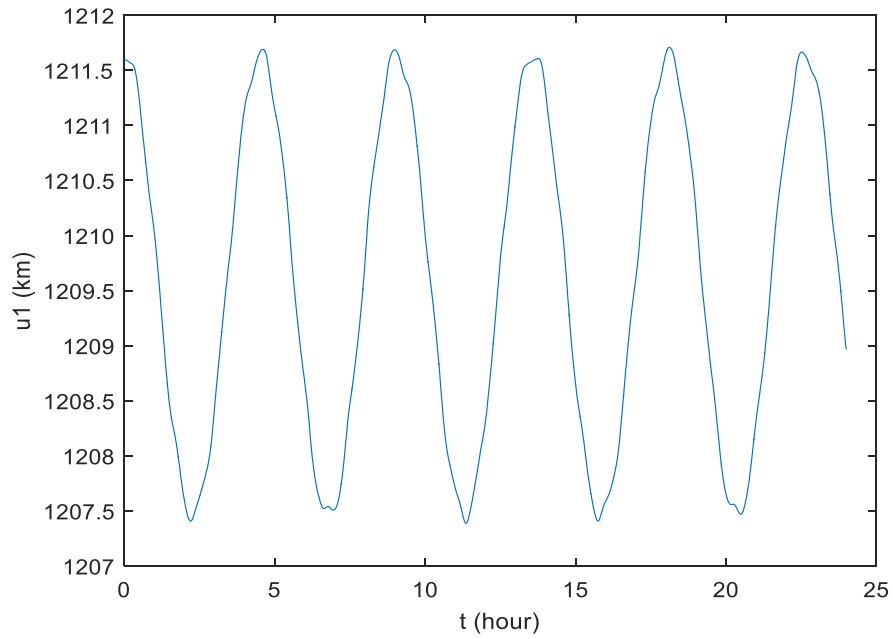


Figure 4.3: Longitudinal Oscillation of the Space Station (u_1) for $m_s = 50$ tons ($T_s=4.53$ hours, $A_s = 2.2$ km)

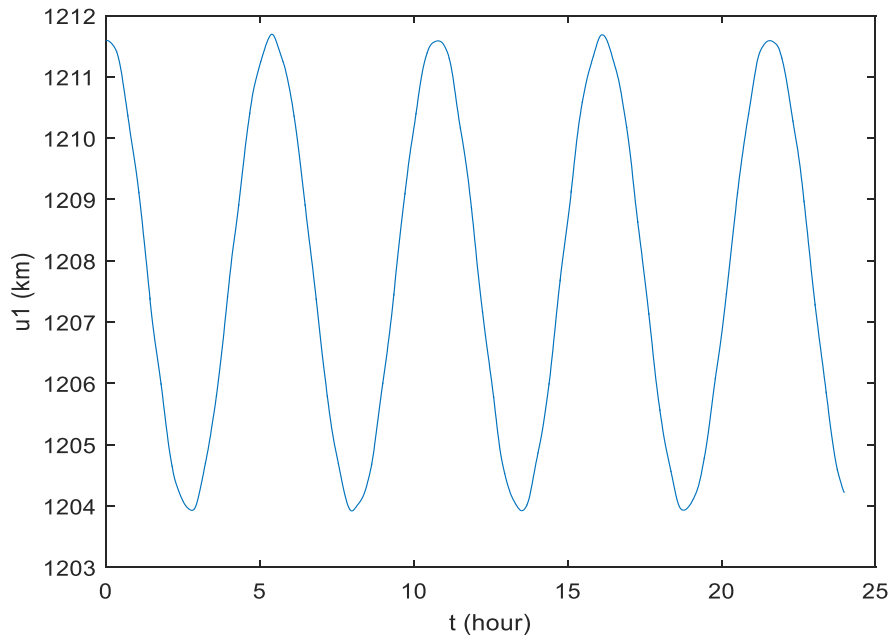


Figure 4.4: Longitudinal Oscillation of the Space Station (u_1) for $m_s = 500$ tons ($T_s = 5.33$ hours, $A_s = 3.85$ km)

This lengthening of periods of oscillation could be attributed to the increase in total mass of the system, which results in a decrease in its frequency of oscillation.

Table 4.1: Period of Space Station Oscillation versus its Mass.

m_s (ton)	50	100	200	300	400	500
T_s (hour)	4.53	4.61	4.80	5.00	5.27	5.33

4.3 The Effect of the Mass of the Space Station (m_s) on its Amplitude of Oscillation(A_s)

It is expected that if the deviation of the space station from the geosynchronous orbit is not considerable, the mass of the space station could have a negligible effect on its amplitude of oscillation.

The second observation is that as the mass of the space station is increased, the amplitude of its longitudinal oscillation increases. For example, when the mass of the space station is set to 50 tons, the amplitude of its longitudinal oscillation was about 2.2 km. But when the mass of the space station is set to 500 tons, the amplitude of its longitudinal oscillation was about 3.85 km (Figures 3.3 and 3.4). The results are shown in Table 4.2.

Table 4.2: Amplitude of Space Station Oscillation (A_s) versus its Mass (m_s)

m_s (ton)	50	100	200	300	400	500
A_s (km)	2.2	2.3	2.65	3	3.4	3.85

This observation can be explained by the fact that any deviation of the space station from the geostationary orbit due to oscillation could bring about an external force on the system, and this force is proportional to the mass of the space station. The value of this transmitted external force can be defined by this equation:

$$F_T = m_s \left[r\Omega^2 - \frac{\mu}{r^2} \right] \quad (4.2)$$

where r is the radial distance of the space station from the center of the earth.

4.4 The Effect of the Mass of the Counterweight (m_c) on the Amplitude of Space Station Oscillations (A_s)

4.4.1 ± 10 Percent Change in the Mass of the Counterweight

In the next step of analysis, the mass of the counterweight was varied, leaving the length of the ribbon unchanged. The goal was to observe the effect of decreasing or increasing the mass of the counterweight by a small percentage on the amplitude of the oscillation of the space station. Accordingly, first the mass of the counterweight was set to 300 tons (a 10% decrease from the nominal value) and the mass of the space station was chosen as 200 tons. The plots were produced, and it was observed that the amplitude of the oscillation of the space station with respect to the GEO (u_{1H}) increased from 2.65 km to about 90 km. The oscillations were pointing toward the earth such that the maximum displacement of the oscillation was at the geostationary orbit (Figure 4.6).

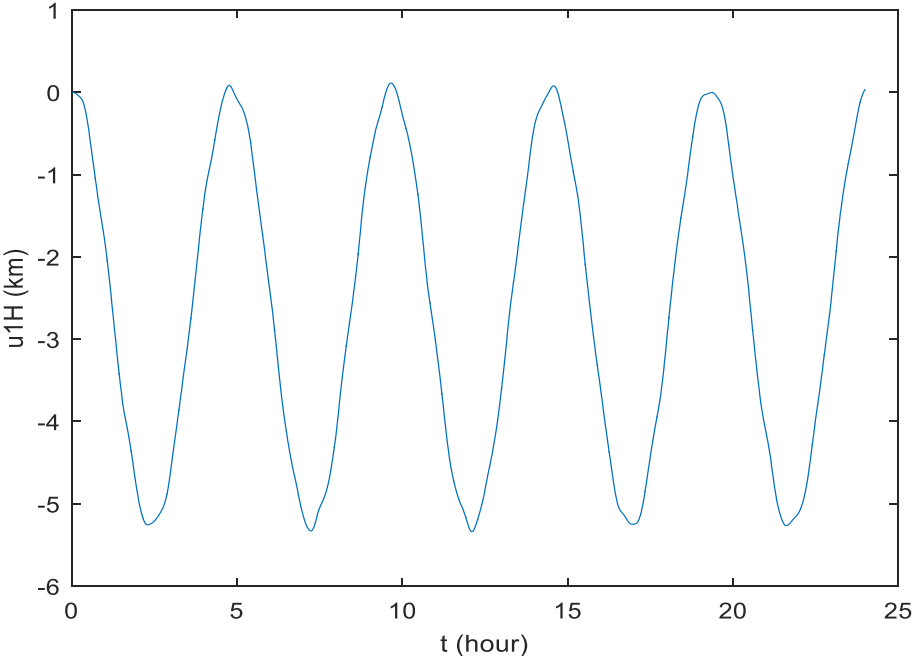


Figure 4.5: Relative Oscillation of the Space Station with Respect to GEO (u_{1H}) for $m_s = 200$ tons; $m_c = 330$ tons.

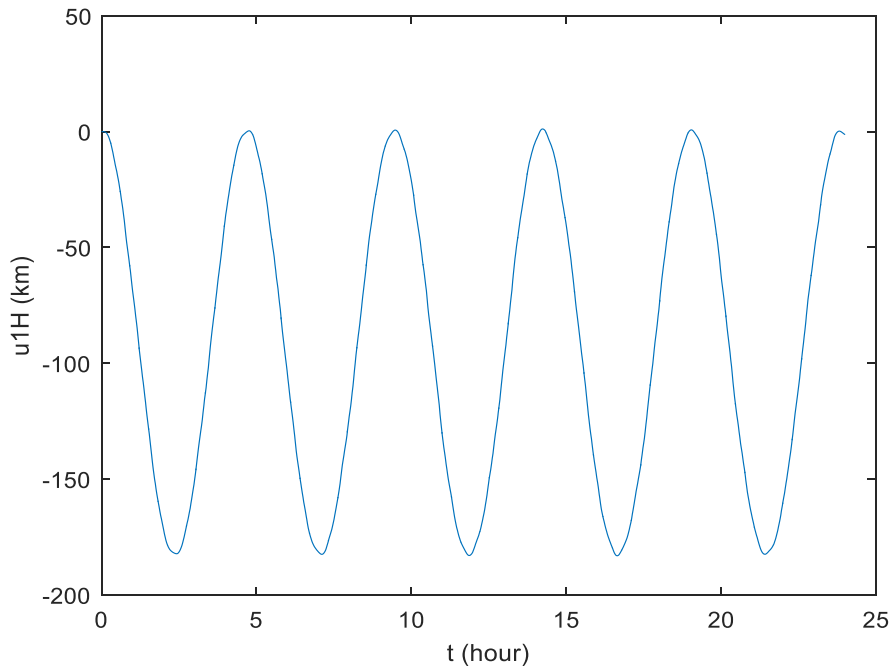


Figure 4.6: Relative Oscillation of the Space Station with Respect to GEO (u_{1H}) for $m_s = 200$ tons; $m_c = 300$ tons (10% decrease).

The mass of the counterweight was then increased by almost 10%, to 360 tons, while the mass of the space station was kept at 200 tons, and the total length of the ribbon remained unchanged. The plots were produced, and it was observed that the amplitude of the oscillation of the space station with respect to the GEO (u_{1H}) increased from 2.65 km to about 87 km. The oscillations were pointing toward space such that the minimum displacement of the oscillation was at the geostationary orbit (Figure 4.7).

It has already been shown that the mass of the counterweight depends strongly on the total length of the ribbon (Equation 4.1). If the mass of the counterweight is even slightly off, it will cause the system to lose equilibrium, and will result in significant oscillation of the space station.

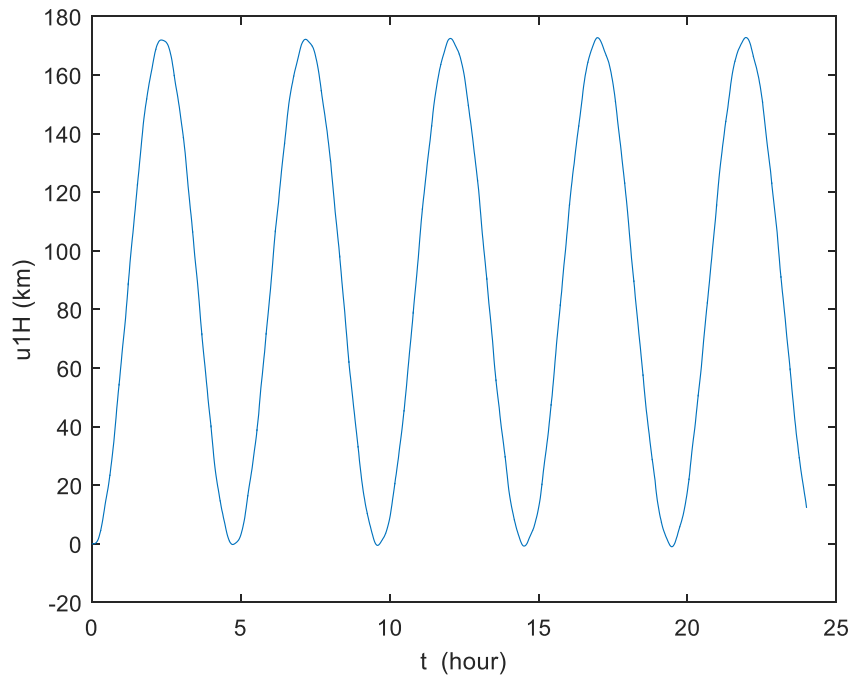


Figure 4.7: Relative Oscillation of the Space Station with Respect to GEO (u_{1H}) for $m_s = 200$ tons; $m_c = 360$ tons (10% increase).

4.4.2 ± 5 Percent Change in the Mass of the Counterweight

To observe the effect of the mass of the counterweight on the amplitude of the space station oscillation more precisely, the plots were repeated for a 5% increase and a 5% decrease in the mass of the counterweight.

It is observed that with a 5% decrease in the mass of the counterweight, the amplitude of the space station oscillation with respect to GEO (u_{1H}) increases from 2.65 km to 52 km. The induced oscillations were pointing toward the earth such that the maximum points of the oscillations are on the GEO.

It is observed that with a 5% increase in the mass of the counterweight, the amplitude of the space station oscillation with respect to GEO (u_{1H}) increases from 2.65 km to 47 km. The induced oscillations were pointing toward space such that the minimum points of the oscillations are on the GEO (Figures 4.8 and 4.9).

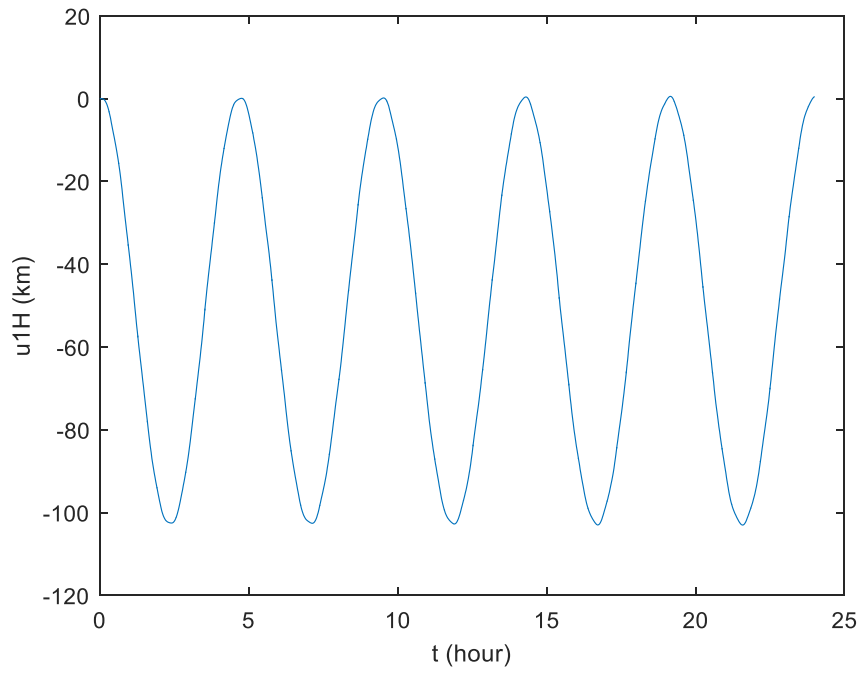


Figure 4.8: Relative Oscillation of the Space Station with Respect to GEO (u_{1H}) for $m_s = 200$ tons; $m_c = 313.5$ tons (5% decrease).

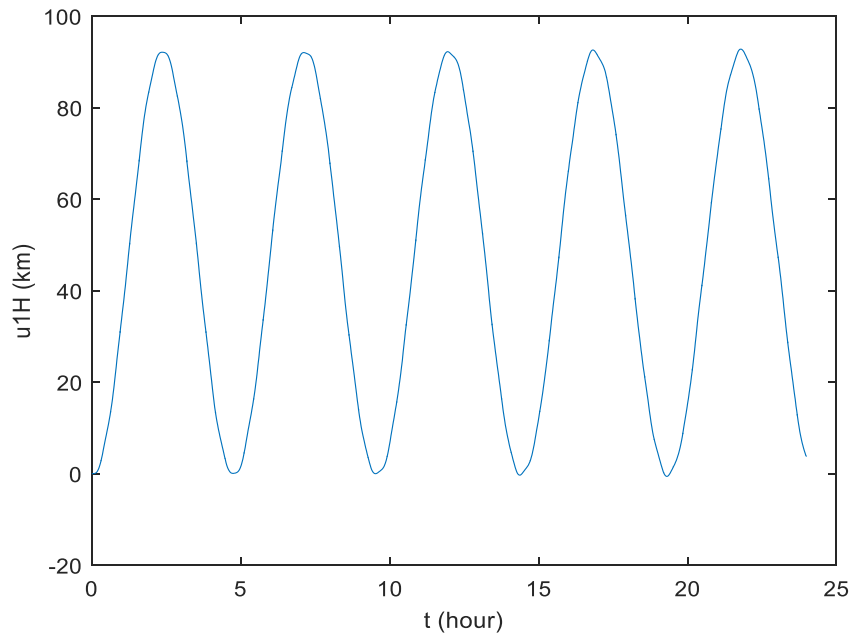


Figure 4.9: Relative Oscillation of the Space Station with Respect to GEO (u_{1H}) for $m_s = 200$ tons; $m_c = 313.5$ tons (5% decrease).

In fact, none of the choices of counterweight mass caused the oscillation trajectory to cross the GEO.

It can be concluded that if the mass of the counterweight is less than the value needed for equilibrium, the induced oscillations of the space station point toward the earth. On the other hand, if the mass of the counterweight is more than the value needed for equilibrium, the induced oscillations of the space station point toward space.

This fact shows that during the construction phase of the space elevator it is necessary to increase the mass of the counterweight while increasing the length of the total ribbon based on equation 4.1 to avoid unexpected oscillations of the space station. In fact, a proper matching between the mass of the counterweight and the total length of the ribbon is the most critical condition for the equilibrium of the system.

4.5 The Effect of the Mass of the Climber (m_e) on the Amplitude of Space Station Oscillations(A_s)

Since the climber is not located at the geosynchronous orbit, it is expected to exert a disturbance on the space elevator. This force is proportional to the mass of the climber, and also depends on the radial distance of the climber from the center of the earth. If the climber is moving along the ribbon, it induces a Coriolis force in the lateral direction too. However, in our model it has been assumed that the climber is stationary at a point along the lower ribbon.

The force exerted by the presence of the climber on the ribbon can change the amplitude of the space station oscillation. If the climber is located on the upper ribbon, the net induced force is positive (pointing toward space), and increases the amplitude of the space station oscillation toward space. On the other hand, if the climber is located on the lower ribbon, the net induced force is negative (pointing toward the earth), and increases the amplitude of the space station toward the earth.

The induced force exerted by the climber is given by equation 4.3.

$$F_e = m_e \left[(R + d_e) \Omega^2 - \frac{\mu}{(R + d_e)^2} \right] \quad (4.3)$$

where m_e is the mass of the climber and d_e is the distance of the climber from the surface of the Earth.

The oscillation of the space station with respect to the geosynchronous orbit is plotted for three choices of the climber mass (100 kg, 500 kg, and 1000 kg), (Figures 4.10, 4.11, and 4.12). In these three cases, the mass of the counterweight and the total length of the ribbon are those needed for equilibrium ($m_c = 330 \text{ tons}, L = 100000 \text{ km}$). The mass of the space station was set to 200 tons, and the climber was located at $d_e = 20000 \text{ km}$.

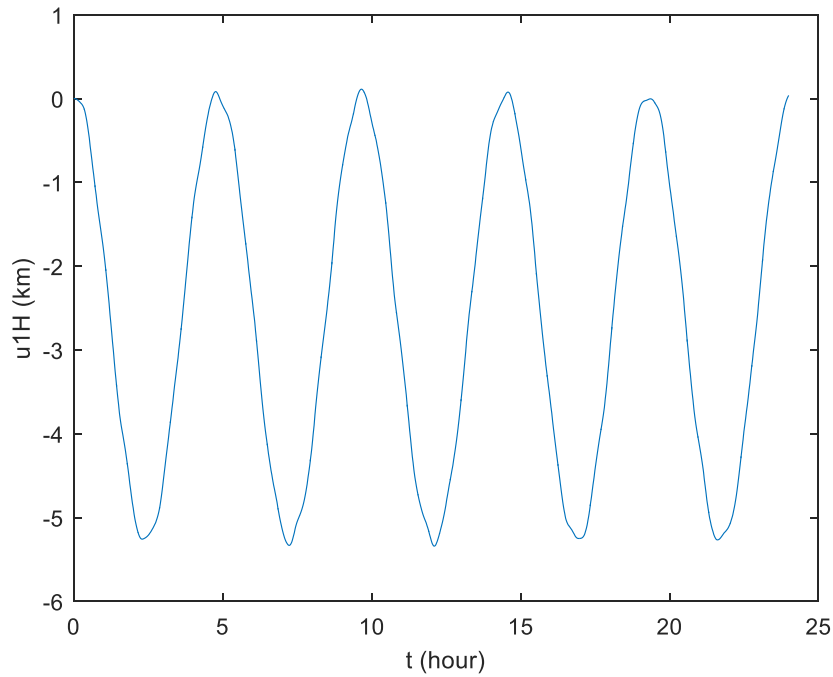


Figure 4.10: Oscillation of the Space Station Relative to the GEO versus time for $m_e = 100 \text{ kg}$.

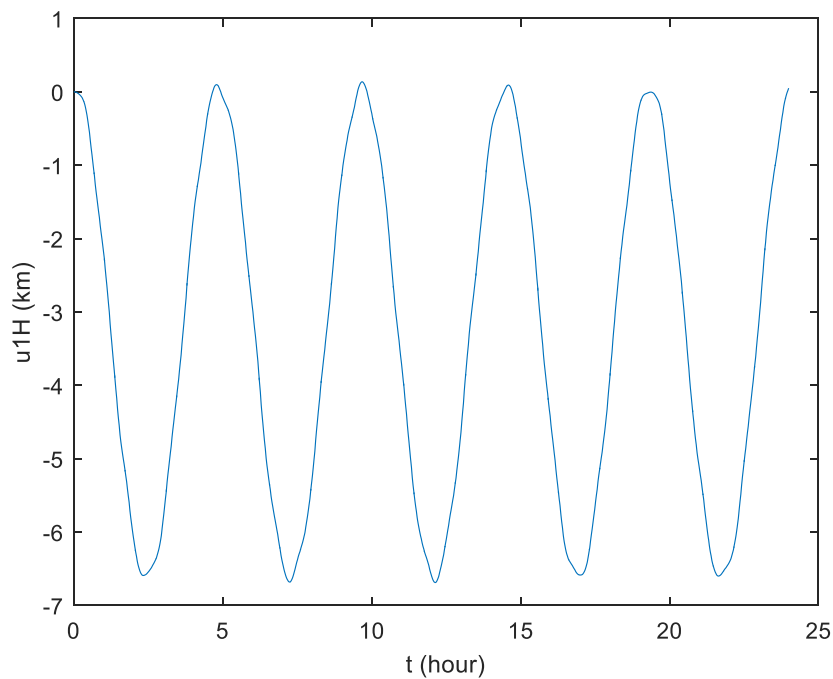


Figure 4.11: Oscillation of the Space Station Relative to the GEO versus time for $m_e = 500 \text{ kg}$.

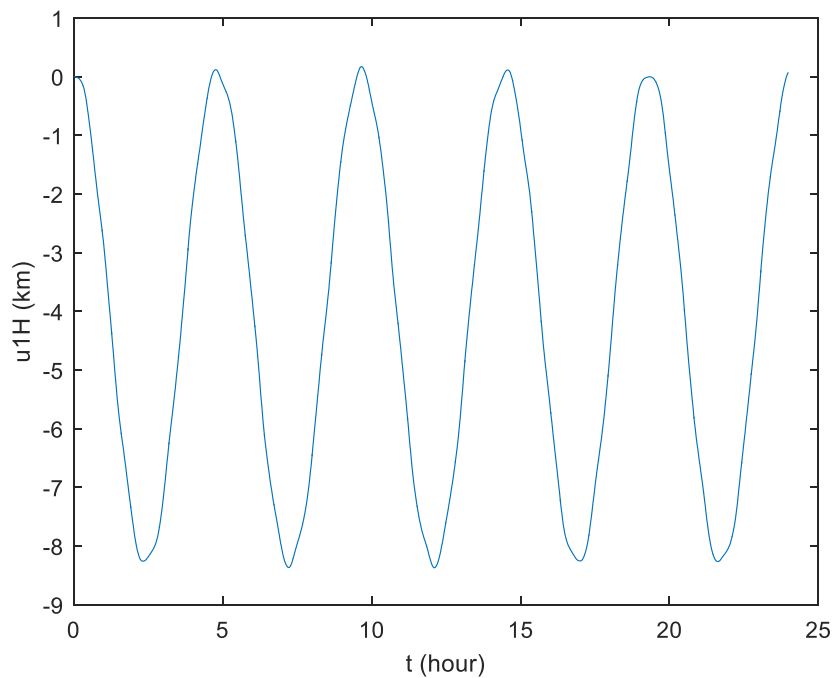


Figure 4.12: Oscillation of the Space Station Relative to the GEO versus time for $m_e = 1000 \text{ kg}$.

The plots show that if the mass of the climber increases, the amplitude of the space station oscillation increases. However, the effect of the mass of the climber on the amplitude of the space station oscillation is not as significant as the effect of the mass of the counterweight. The summary of these results is shown in Table 4.3.

Table 4.3: Amplitude of the Space Station Oscillation (A_s) Versus the Mass of the Climber (m_e).

m_e (kg)	100	500	1000
A_s (km)	2.65	3.35	4.15

4.6 The Effect of the Climber Position on the Space Elevator Equilibrium

The climber as a point mass exerts an external force on the space elevator. The value of this force is proportional to the climber mass, and also depends on the distance of the climber from the surface of the earth. If the climber is located on the upper ribbon, the direction of the force is pointed toward space. But, if the climber is located on the lower ribbon, the direction of this force is pointed toward the earth (Equation 4.3).

In our model, it was assumed that the climber was located at a point along the lower ribbon. It was shown that the force induced by the climber would result in an increase in the amplitude of the space station toward Earth. It is believed that with a small percentage increase in the mass of the counterweight, this induced force could be avoided.

$$\sum F_{net} = 0 \quad (4.4)$$

$$\Delta m_c \left[(R + L)\Omega^2 - \frac{\mu}{(R+L)^2} \right] + m_e \left[(R + d_e)\Omega^2 - \frac{\mu}{(R+d_e)^2} \right] = 0 \quad (4.5)$$

Where Δm_c is the needed increment in the mass of the counterweight.

Using the equation $\Omega^2 = \frac{\mu}{R_G^3}$ and after some algebra we have:

$$r_e^{\Delta c} = \frac{\Delta m_c}{m_e} = \left(\frac{R+L}{R+d_e} \right) \left[\frac{R_G^3 - (R+d_e)^3}{(R+L)^3 - R_G^3} \right] \quad (4.6)$$

Where $r_e^{\Delta c}$ is the ratio of required increment of the counterweight mass to the mass of the climber. Having defined the total length of the ribbon, this ratio depends only on the distance of the climber from the surface of the earth (d_e).

The plot of $r_e^{\Delta c}$ versus d_e is presented in Figure 4.13. However, considering the small mass of the climber compared to the mass of the counterweight, the required adjustment in the mass of the counterweight is small.

Considering the needed adjustment in the mass of the counterweight, equation 4.1 is modified here (Equation 4.7):

$$m_c = \gamma A_m h \frac{\exp[F(s)]|_{s=L_0}}{\left(\frac{R}{R_G}\right)^2 \left[\frac{R+L}{R_G} - \left(\frac{R_G}{R+L}\right)^2\right]} + r_e^{\Delta c} \cdot m_e \quad (4.7)$$

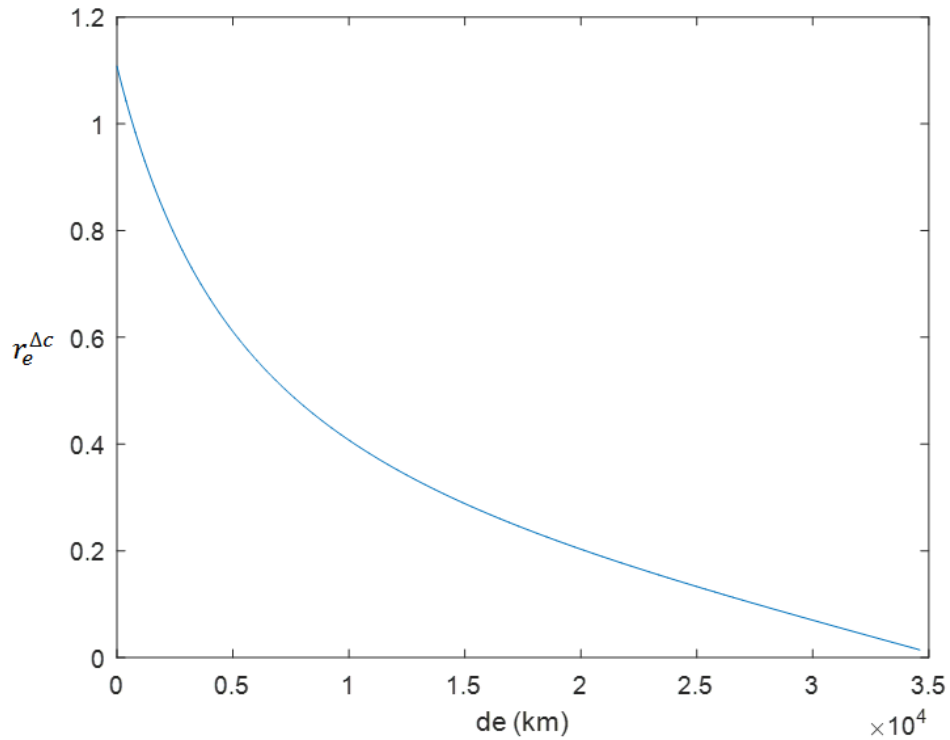


Figure 4.13: Plot of $r_e^{\Delta c}$ versus d_e .

4.7 Oscillation of the Space Station with Non-zero Initial Displacement

In the last part of the analysis, the initial values of the generalized coordinates were set in a way such that the initial position of the space station would be almost 40 km above the geosynchronous

orbit. But all the initial velocities were set to zero. The mass of the space station was set to 200 tons. The mass of the counterweight was set to 330 tons to be compatible with the total length of the ribbon (100000 km), and maximum cross sectional area of the ribbon (10 mm^2). The goal was to observe the effect of this initial condition on the oscillation of the space station with respect to the geosynchronous altitude, and compare it to the case when the initial position of the space station is on the geosynchronous orbit.

It was observed that compared to the case when all the initial conditions are zero, the oscillations of the space station now cross the geosynchronous orbit. The maximum displacement above the geosynchronous orbit was 42 km, and the maximum displacement below the geosynchronous altitude was 50 km (Figure 4.14). As a result, the amplitude of oscillations of the space station was found to be 46 km. For similar design parameters, when the initial position of the space station was on the geosynchronous altitude and the initial velocity was zero, we had found that the amplitude of the space station oscillation was just 2.65 km.

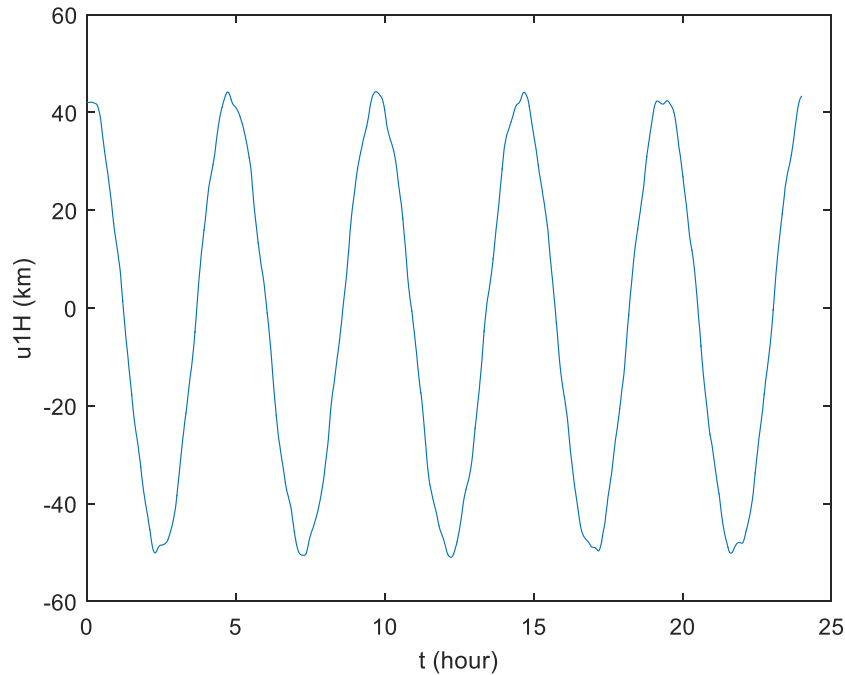


Figure 4.14: Oscillation of the Space Station relative to GEO with initial Position of 40 km above the GEO.

4.8 Summary of Results

The main findings of this analysis are summarized in Table 4.4. The total length of the ribbon after elongation in all cases as shown is $L = 100000 \text{ km}$, and the maximum cross sectional area of the ribbon is $A_m = 10 \text{ mm}^2$. As discussed before, these values are consistent with the mass of the counterweight at about 330 tons. The results for $\pm 5\%$ and $\pm 10\%$ changes in the mass of the counterweight are also shown in this table.

Table 4.4: Summary of the Results for the Oscillation of Space Station and Counterweight

$m_c \text{ (ton)}$	$m_s \text{ (ton)}$	$T_s \text{ (hour)}$	$A_s \text{ (km)}$	$A_c \text{ (km)}$
330	50	4.53	2.2	2
330	100	4.61	2.3	2.25
330	200	4.80	2.65	2.65
330	300	5.00	3	3
330	400	5.27	3.4	3.45
330	500	5.33	3.85	3.95
300 (~10% decrease)	200	4.80	90	90
313.5 (5% decrease)	200	4.80	52	51
346.5 (5% increase)	200	4.87	47	47
360 (~10% increase)	200	4.90	87	88

Here, A_s is the amplitude of the space station oscillation, and A_c is the amplitude of the counterweight oscillation.

CHAPTER 5: CONCLUSIONS

5.1 Summary of the Results

In this study, the longitudinal oscillations of the space elevator ribbon was examined. We had the following findings:

- 1) The period of the oscillations of the ribbon depends on the mass of the space station. It was shown that by increasing the mass of the space station, its period of oscillation increases too. This increase in the period of oscillation could be attributed to the resulting increase in the total mass of the space elevator. Any increase in the total mass will decrease its frequency of oscillation.
- 2) The amplitude of space station oscillation depends on its mass. In fact, by increasing the mass of the space station the amplitude of its oscillation increases too. This finding can be explained by the fact that when the space station is not on the geosynchronous orbit, an external force proportional to its mass will be transmitted to it.
- 3) The mass of the counterweight has a significant effect on the amplitude of the space station oscillation. Depending on the total length of the ribbon after elongation, and its maximum cross sectional area, an accurate value for the mass of the counterweight should be chosen. Any small change in the mass of the counterweight will result in significant oscillation and an increase in the amplitude of space station oscillation. It was found that any decrease in the mass of the counterweight would result in significant oscillation of the space station toward the earth, such that the maximum points of the oscillation trajectory are on the geosynchronous orbit.

On the other hand, it was found that any increase in the mass of the counterweight will result in significant oscillation of the space station toward space, such that the minimum points of the oscillation trajectory are on the geosynchronous orbit.

It was found that none of the choices of counterweight mass caused the trajectory of space station oscillation to cross the geosynchronous orbit. In all cases, the trajectory of space station oscillation is tangent to the geosynchronous orbit, either at its maximum or minimum points.

- 4) Regardless of the mass of the space station and the mass of the counterweight, the oscillation of the lower ribbon has a more significant amplitude than the upper ribbon. As

a result, the oscillation of the counterweight, which is the superposition of the oscillation of the lower and upper ribbons, is mostly due to the oscillation of the lower ribbon.

Finally, the amplitude and the period of space station oscillation, and also the amplitude of counterweight oscillation for several space station and counterweight mass choices were found.

- 5) The effect of the mass of the climber on the amplitude of space station oscillation was studied too. It was shown that by increasing the mass of the climber, the amplitude of space station oscillation increases by a small percentage.
- 6) The effect of the position of the climber on space elevator equilibrium was examined. The needed adjustment to the mass of the counterweight as a function of the position of the climber was found.

5.2 Suggestions for Future Study

In this study, only the longitudinal motion of the space elevator components was considered. Important dynamics such as the lateral motion (two-dimensional), three-dimensional motion, and Coriolis force due to the motion of the climber were not considered. However, as opposed to previous works, the space station was added to the model.

Therefore, it is suggested that the effect of the space station's mass and that of the counterweight be studied for the in-plane motion as well as for the three dimensional.

It is also suggested that the dynamics of the space elevator for a case in which the climber is located on the upper ribbon be studied, along with the effect of the climber's mass, its distance from the geosynchronous orbit, and its speed in relation to the oscillation of the space station.

REFERENCES

- Artsutanov, Y., (1960) "To the Cosmos by Electric Train," *Komsomolskaya Parvda* (translated from Russian).
- Cohen, S., & Misra, A. K. (2015). Static deformation of space elevator tether due to climber. *Acta Astronautica*, *111*, 317-322. doi: <http://dx.doi.org/10.1016/j.actaastro.2015.02.017>
- Cohen, S. S., & Misra, A. K. (2007). Elastic oscillations of the space elevator ribbon. *Journal of Guidance Control and Dynamics*, *30*(6), 1711-1717. doi: 10.2514/1.29010
- Cohen, S. S., & Misra, A. K. (2009). The effect of climber transit on the space elevator dynamics. *Acta Astronautica*, *64*(5-6), 538-553. doi: <http://dx.doi.org/10.1016/j.actaastro.2008.10.003>
- Edwards, B. C. (2000). Design and deployment of a space elevator. *Acta Astronautica*, *47*(10), 735-744. doi: Doi 10.1016/S0094-5765(00)00111-9
- Fujii, H. A. (2013). *Dynamics of space elevator and its features*. Paper presented at the Proceedings of the International Astronautical Congress, IAC.
- Iijima, S. (1991). Helical microtubules of graphitic carbon. *nature*, *354*(6348), 56-58.
- Lang, D. D. (2005). Space elevator dynamic response to in-transit climbers. *proceedings of the Space Engineering and Space Institute*.
- Meirovitch, L. (1980). *Computational methods in structural dynamics* (Vol. 5): Springer Science & Business Media.
- Pearson, J. (1975). Orbital Tower: A Spacecraft Launcher Using the Earth's Rotational Energy. *Acta Astronautica*, *2*(9-10), 785-799.
- Pearson, J. (2005). Konstantin Tsiolkovski and the origin of the space elevator. *AAS History Series*, *26*, 17-24.
- Tsiolkovsky, K. E., (1985) "Grezi o zemle I nene," *U.S.S.R. Academy of Sciences*, pp. 35 (in Russian, "Day-Dreams of Heaven and Earth," reprinted in 1959).
- Williams, P. (2009). Dynamic multibody modeling for tethered space elevators. *Acta Astronautica*, *65*(3-4), 399-422. doi: <http://dx.doi.org/10.1016/j.actaastro.2008.11.016>
- Williams, P., & Ockels, W. (2010). Climber motion optimization for the tethered space elevator. *Acta Astronautica*, *66*(9-10), 1458-1467. doi:10.1016/j.actaastro.2009.11.003
- Woo, P., & Misra, A. K. (2010). Dynamics of a partial space elevator with multiple climbers. *Acta Astronautica*, *67*(7-8), 753-763. doi:10.1016/j.actaastro.2010.04.023